Cell

FOXO/4E-BP Signaling in *Drosophila* Muscles Regulates Organism-wide Proteostasis during Aging

Fabio Demontis[1,*] and Norbert Perrimon[1,2,*]
[1]Department of Genetics
[2]Howard Hughes Medical Institute
Harvard Medical School, 77 Avenue Louis Pasteur, Boston, MA 02115, USA
*Correspondence: fdemontis@genetics.med.harvard.edu (F.D.), perrimon@receptor.med.harvard.edu (N.P.)
DOI 10.1016/j.cell.2010.10.007

SUMMARY

The progressive loss of muscle strength during aging is a common degenerative event of unclear pathogenesis. Although muscle functional decline precedes age-related changes in other tissues, its contribution to systemic aging is unknown. Here, we show that muscle aging is characterized in *Drosophila* by the progressive accumulation of protein aggregates that associate with impaired muscle function. The transcription factor FOXO and its target 4E-BP remove damaged proteins at least in part via the autophagy/lysosome system, whereas *foxo* mutants have dysfunctional proteostasis. Both FOXO and 4E-BP delay muscle functional decay and extend life span. Moreover, FOXO/4E-BP signaling in muscles decreases feeding behavior and the release of insulin from producing cells, which in turn delays the age-related accumulation of protein aggregates in other tissues. These findings reveal an organism-wide regulation of proteostasis in response to muscle aging and a key role of FOXO/4E-BP signaling in the coordination of organismal and tissue aging.

INTRODUCTION

Aging of multicellular organisms involves distinct pathogenic events that include higher mortality, the progressive loss of organ function, and susceptibility to degenerative diseases, some of which arise from protein misfolding and aggregation. Recent genetic studies in the mouse, the nematode *Caenorhabditis elegans*, and the fruitfly *Drosophila melanogaster* have expanded our understanding of the evolutionarily conserved signaling pathways regulating aging, with the identification of several mutants that have prolonged or shortened life spans (Kenyon, 2005). Manipulation of longevity-regulating pathways in certain tissues is sufficient to extend life expectancy, indicating that some tissues have a predominant role in life span extension (Libina et al., 2003; Wang et al., 2005; Wolkow et al., 2000). For example, *foxo* overexpression in the *Drosophila* fat body extends life span, indicating a key role of this tissue in the regulation of longevity (Giannakou et al., 2004; Hwangbo et al., 2004). In addition, because most tissues undergo progressive deterioration during aging (Garigan et al., 2002), it is thought that organismal life span may be linked to tissue senescence. However, our understanding of the mechanisms regulating tissue aging and their interconnection to life span is limited. For example, analysis in *Drosophila* has revealed that the prevention of age-dependent changes in cardiac performance does not alter life span (Wessells et al., 2004), raising the possibility that functional decline in distinct tissues may have different outcomes on the systemic regulation of aging.

The Insulin/IGF-1 signaling pathway has been implicated in the control of aging across evolution via its downstream signaling component FOXO (DAF-16 in *C. elegans*), a member of the fork-head box O transcription factor family (Salih and Brunet, 2008). FOXO regulates the expression of a series of target genes involved in metabolism, cell growth, cell proliferation, stress resistance, and differentiation via direct binding to target gene promoter regions (Salih and Brunet, 2008). Mutations in *foxo/daf-16* reduce life span and stress resistance in both *C. elegans* and flies, indicating a key role in organism aging (Junger et al., 2003; Salih and Brunet, 2008). In addition to regulating life span, FOXO has been reported to prevent the pathogenesis of some age-related diseases. For example, FOXO reduces the toxicity associated with aggregation-prone human mutant Alzheimer's and Huntington's disease proteins (proteotoxicity) in *C. elegans* and mice, suggesting that regulating protein homeostasis (proteostasis) during aging may have a direct effect on the pathogenesis of human neurodegenerative diseases (Cohen et al., 2006; Hsu et al., 2003; Morley et al., 2002). However, little is known on the protective mechanisms induced in response to FOXO signaling and whether they vary in different aging tissues and disease contexts.

Among the plethora of age-related pathological conditions, the gradual decay in muscle strength is one of the first hallmarks of aging in many organisms, including *Drosophila*, *C. elegans*, mice and, importantly, humans (Augustin and Partridge, 2009; Herndon et al., 2002; Nair, 2005; Zheng et al., 2005). However, despite its medical relevance, the mechanisms underlying muscle aging are incompletely understood. Functional changes in skeletal muscles temporally precede the manifestation of
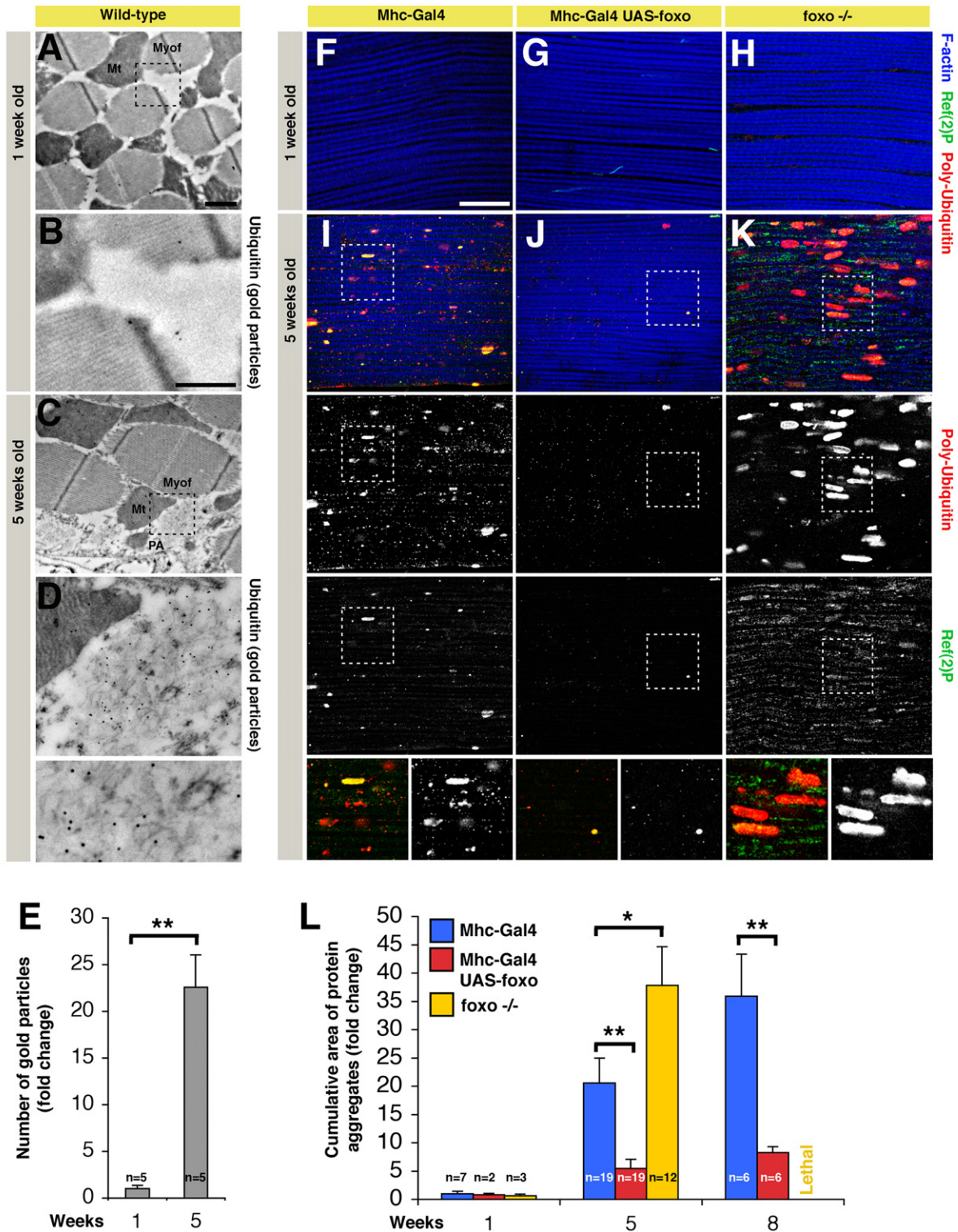
Cell

Figure 1. FOXO Signaling in Skeletal Muscles Preserves Proteostasis during Aging

(A–D) Electron micrographs of immunogold-labeled *Drosophila* skeletal muscles of wild-type flies at one (A and B) and 5 weeks of age (C and D). Protein aggregates (PA) are detected in the cytoplasm in proximity to mitochondria (Mt) and myofibrils (Myof) in old (C and D) but not young flies (A and B). Numerous gold particles (indicative of anti-ubiquitin immunoreactivity) localize to filamentous structures at 5 weeks of age (C and D), while only a few are present in muscles from young flies. Scale bars are 1 μm (A and C) and 500 nm (B and D).

Cell

aging in other tissues (Herndon et al., 2002), and reduced muscle strength is associated with an increased risk in developing Alzheimer's and Parkinson's diseases (Boyle et al., 2009; Chen et al., 2005). However, although aging-related changes in skeletal muscles have been proposed to affect physiological processes in distal organs (Nair, 2005), whether or not muscle senescence modulates the pathogenesis of degenerative events in other tissues is unknown.

The fruit fly *Drosophila* is an excellent model to study muscle aging. The progressive decline in muscle strength and function observed in humans is recapitulated in this system (Rhodenizer et al., 2008), which is amenable to extensive genetic manipulation. By using this model organism, we have searched for the molecular mechanisms responsible for muscle aging and found that decreased protein quality control plays a role in the pathogenesis of age-related muscle weakness. Interestingly, increased activity of the transcription factor FOXO and its target Thor/4E-BP are sufficient to delay this process and preserve muscle function at least in part by promoting the basal activity of the autophagy/lysosome system, an intracellular protein degradation pathway that removes aggregates of the damaged proteins (Rubinsztein, 2006).

Moreover, we report that FOXO/4E-BP signaling in muscles extends life span and regulates proteostasis organism-wide by regulating feeding behavior, release of insulin from producing cells, and *4E-BP* induction in nonmuscle tissues. Thus, we propose a model by which FOXO/4E-BP signaling in muscles preserves systemic proteostasis by mimicking some of the protective effects of decreased nutrient intake.

RESULTS

Loss of Proteostasis during Muscle Aging Is Prevented by FOXO

To detect cellular processes that are responsible for decreased muscle strength in aging flies, we monitored cellular changes in indirect flight muscles of wild-type flies by immunogold-electron microscopy (IEM). In older flies, we detected filamentous cytoplasmic structures that were instead absent in muscles from young flies (Figures 1A–1D). Filamentous materials present in these structures stained with an anti-ubiquitin antibody (Figure 1D), a marker for proteins that are polyubiquitinated, suggesting that the cytoplasmic structures are aggregates of damaged proteins. Aggregates were variable in size and were detected in both resin-embedded sections (Figure 1) and cryosections (data not shown) of thoracic muscles of the old but not the young flies, in parallel with an increase in the overall

number of gold particles (Figure 1E). To test the hypothesis that muscle function during aging may decrease due to defects in protein homeostasis, we better characterized the age-related deposition of protein aggregates by immunofluorescence. In agreement with the IEM analysis (Figures 1A–1E), we observed that aging skeletal muscles progressively accumulate aggregates of polyubiquitinated proteins (ranging up to several μm) that colocalize with p62/Ref(2)P, an inclusion body component (Figures 1F and1I). The cumulative area of protein aggregates increases during aging (Figure 1L), suggesting that the progressive protein damage, together with a decrease in the turnover of muscle proteins, may result in the age-related decline of muscle strength.

To better characterize how protein quality control is linked with aging in muscles, we analyzed the deposition of protein aggregates in syngenic flies with *foxo* overexpression. *Foxo* overexpression results in its activation (Giannakou et al., 2004; Hwangbo et al., 2004) and was achieved specifically in muscles via the UAS-Gal4 system using the Mhc-Gal4 driver (see Figure S1 available online). Increased FOXO activity in muscles did not affect developmental growth and differentiation (as estimated by body weight and sarcomere assembly) (Figure S2), and resulted in the delayed accumulation of aggregates containing polyubiquitinated proteins and Ref(2)P during aging (Figures 1G and 1J, compare with control muscles in Figures 1F and 1I). Next, we tested whether *foxo* null animals display accelerated muscle aging, and found an increased accumulation of protein aggregates (Figures 1H and1K), indicating that FOXO is both necessary and sufficient to modulate muscle proteostasis (Figure 1L).

To further corroborate these findings, we overexpressed either the wild-type or the constitutive-active *foxo* transgenes using the Dmef2-Gal4 muscle driver in combination with the temperature-sensitive tubulin-Gal80[ts] transgene to achieve adult-onset *foxo* overexpression in muscles (Figure S3). Transgene overexpression significantly preserved muscle proteostasis in both cases, while the controls displayed an increased accumulation of protein aggregates (Figure S3). All together, these results indicate that protein homeostasis depends on FOXO activity during muscle aging.

4E-BP Controls Proteostasis in Response to Pten/FOXO Activity

To dissect the stimuli that encroach on FOXO to control proteostasis, we tested whether *Pten* overexpression phenocopies FOXO activation. Consistent with its role in activating FOXO, we found that Pten decreased the accumulation of protein

(E) The number of gold particles, indicative of ubiquitin immunoreactivity, significantly increases in old age (standard error of the mean [SEM] is indicated with n; **p < 0.01).

(F–L) Immunostaining of indirect flight muscles from flies with (*UAS-foxo*/+;*Mhc-Gal4*/+) or without (*Mhc-Gal4*/+) *foxo* overexpression at 1 week (F and G) and 5 weeks of age (I and J), and *foxo* homozygous null (*MhcGal4, foxo*[21/25]) flies (H and K). Polyubiquitin (red) and p62/Ref(2)P (green) immunoreactivities reveal an increased deposition of aggregates containing polyubiquitin proteins during aging in muscles of control flies (F and I), and, to a lesser extent, in muscles overexpressing *foxo* (G and J). Conversely, muscles from *foxo* null animals display an accelerated deposition of protein aggregates (H and K) in comparison with controls (F and I). Note the significant increase in the cumulative area of protein aggregates (indicative of both aggregate size and number) in (K) versus (I), and in (I) versus (J), indicating that the dentrol of protein homeostasis is linked to FOXO activity in muscles (quantification in [L]) (SEM is indicated with n; *p < 0.05, **p < 0.01). Representative polyubiquitin and Ref(2)P immunoreactivities are shown in insets. Phalloidin staining (blue) outlines F-actin, which is a component of muscle myofibrils. Scale bar is 20 μm (F–K).
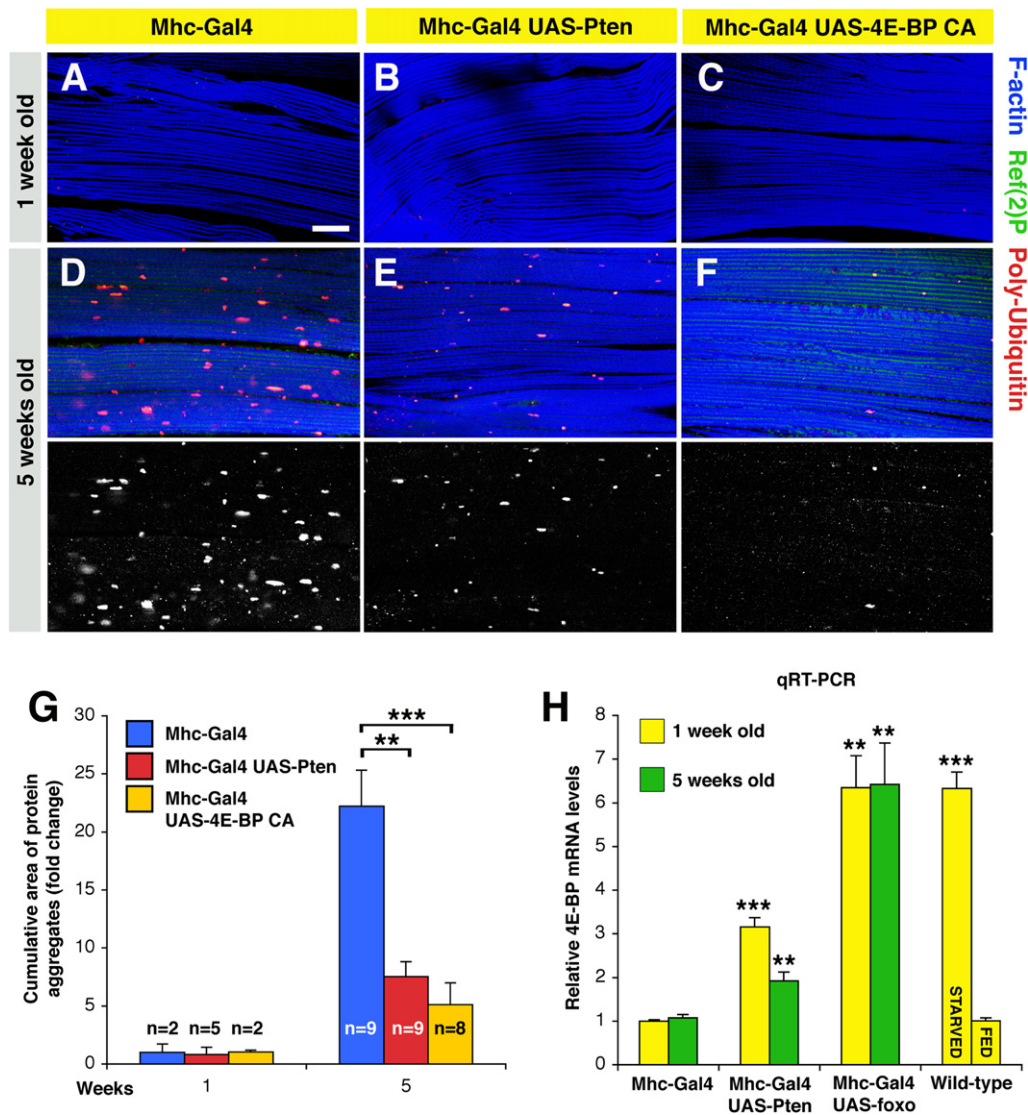
See also Figure S1, Figure S2, and Figure S3.

Cell

Figure 2. 4E-BP Preserves Proteostasis in Response to Pten/FOXO Signaling

(A–F) Immunostaining of muscles overexpressing *Pten* and constitutive active (CA) *4E-BP*. In both cases, a decrease in the accumulation of polyubiquitin protein aggregates is observed at 5 weeks of age in comparison with age-matched controls, suggesting that these interventions can preserve proteostasis in aging muscles. Scale bar is 20 μm. *Hsp70* overexpression has instead limited effects (Figure S4, Table S1, Table S2).

(G) A reduction in the cumulative area of protein aggregates is observed upon increased activity of either Pten or 4E-BP in comparison with controls (SEM is indicated with n; **p < 0.01, ***p < 0.001).

(H) Relative quantification of *Thor/4E-BP* mRNA levels from thoraces of syngenic flies at 1and 5 weeks of age. A significant increase in *4E-BP* expression is detected in response to fasting and Pten and FOXO activity (**p < 0.01, ***p < 0.001; SEM is indicated with n = 4).

aggregates during aging (Figures 2B and 2E; see controls in Figures 2A and 2D).

Next, we examined the responses induced by Pten/FOXO signaling. First, we examined whether FOXO activity delays protein damage by inducing chaperones that are key for protein quality control (Tower, 2009). In response to FOXO activity in muscles, we detected an increase in the mRNA levels of *Hsp70* and its cofactors involved in protein folding (*Hip*, *Hop*, *Hsp40,* and *Hsp90*) but not in protein degradation (*Chip* and *Chap*) (Figure S4 and Table S1). FOXO regulates directly the

expression of *Hsp70* and its cofactors, as estimated with Luciferase transcriptional reporters based on the proximal promoter region of target genes (Figure S4 and Table S2). On this basis, we tested whether *Hsp70* overexpression preserves proteostasis during aging but found little changes in the age-related accumulation of protein aggregates (Figure S4). Thus, we conclude that additional FOXO-dependent responses are involved.

Among the FOXO-target genes, *Thor/4E-BP* has a key role in delaying aging by regulating protein translation (Zid et al., 2009; Tain et al., 2009). However, the cellular mechanisms that

Cell

are regulated by 4E-BP are largely unknown. To test whether 4E-BP controls proteostasis during muscle aging, we overexpressed a constitutive active form of *4E-BP* in muscles and observed limited accumulation of protein aggregates during aging (Figures 2C and 2F)compared with controls (Figures 2A and 2D). All together, increased activity of Pten or 4E-BP significantly decreases the cumulative area of protein aggregates (Figure 2G).

In addition, a significant increase in *4E-BP* mRNA levels is induced in muscles upon *Pten*, *foxo* overexpression, and fasting (Figure 2H). All together, these findings suggest that 4E-BP is key to control proteostasis in response to Pten/FOXO signaling.

FOXO/4E-BP Signaling Regulates Proteostasis via the Autophagy/ Lysosome System

While FOXO/4E-BP signaling mounts a stress resistance response that may decrease the extent of protein damage due to various stressors (Salih and Brunet, 2008; Tain et al., 2009), we wondered whether it regulates the removal of damaged proteins via macroautophagy. In this process, entire regions of the cytoplasm are sequestered in a double membrane vesicle (autophagosome) that subsequently fuses with a lysosome, where the autophagic cargo is degraded (Rubinsztein, 2006). Although the primary role of autophagy is to mount an adaptive response to nutrient deprivation, its basal activity is required for normal protein turnover (Hara et al., 2006). In agreement with this notion, suppression of basal autophagy leads to the accumulation of polyubiquitin protein aggregates in a number of contexts (Korolchuk et al., 2009; Rubinsztein, 2006).

To test whether autophagy is regulated in response to FOXO signaling in muscles, we used a GFP-tagged version of the autophagosome marker Atg5 (Rusten et al., 2004). While the number of Atg5-GFP punctae decreases during aging in control muscles (Figures 3A and 3B), it is in part maintained in response to *foxo* overexpression (Figures 3C and 3D, and quantification in Figure 3E). In addition, given the interconnection between the lysosome system and autophagy, we have monitored a GFP-tagged version of the lysosome marker Lamp1 (lysosome-associated membrane protein 1) and detected an overall increase in the number of GFP punctae in response to overexpression of the autophagy inducer kinase *Atg1*, *foxo*, and *4E-BP CA* in muscles at both 1 and 5 weeks of age (Figures 3G–3I and 3K–3M in comparison with controls in Figures 3F and 3J and quantification in Figure 3N).

Closer inspection revealed that the abundance of Lamp1-GFP vesicles inversely correlates with the progressive deposition of polyubiquitin protein aggregates, suggesting that FOXO/4E-BP signaling regulates proteostasis at least in part via the autophagy/lysosome system. To further test this hypothesis, we analyzed the age-related changes in autophagy gene expression, which have been previously used as a correlative measurement of autophagic activity (Gorski et al., 2003; Simonsen et al., 2008). Interestingly, the expression of several autophagy genes involved in autophagosome induction (*Atg1*), nucleation (*Atg6*), and elongation (*Atg5*, *Atg7*, and *Atg8*) progressively declines during aging in muscles (Figure 3O), suggesting that gene expression changes likely contribute to the accumulation of damaged proteins. Conversely, *foxo* overexpression increased

the basal expression of several *Atg* genes at both young and old age, suggesting that their increased expression contributes to the beneficial effects of FOXO on proteostasis. To test this hypothesis, we knocked down Atg7 levels in *foxo*=overexpressing flies and analyzed the deposition of polyuiquitin protein aggregates. Interestingly, RNAi treatment brought about a ~50% decrease in *Atg7* mRNA levels and resulted in a partial increase in the buildup of insoluble ubiquitinated proteins at 8 weeks, compared with age-matched, mock-treated flies (white RNAi) and 1-week-old flies (Figure 3P).

All together, these findings suggest that FOXO/4E-BP signaling prevents the buildup in protein damage, at least in part by promoting the basal activity of the autophagy/lysosome system.

### Prevention of Muscle Aging by FOXO and 4E-BP Extends Life Span

To evaluate whether preserving proteostasis can prevent functional alterations in aging muscles, we assessed muscle strength with negative geotaxis and flight assays (see Experimental Procedures). As shown in Figures 4A and 4B, muscle functionality gradually decreases in aging flies, resulting in impaired climbing and flight ability. Notably, *foxo* (Figure 4A) and *4E-BP* activity (Figure 4B) significantly preserve muscle strength during aging. Thus, FOXO and 4E-BP prevent both the cellular degenerative events and the functional decay of aging muscles.

Epidemiological studies in humans have associated muscle senescence with increased mortality (Nair, 2005), implying that muscle aging may have organism-wide consequences beyond muscle function. To ask whether the prevention of muscle aging affects the organism life span, we manipulated the activity of components of the Akt pathway in muscles and scored for their effects on viability. As shown in Figures 4C and 4D, either *Pten*, *foxo*, or *4E-BP CA* overexpression in muscles is sufficient to significantly extend longevity by increasing the median and maximum life span. 4E-BP increased life span also in *foxo* heterozygous null animals (Figure 4D), while *Hsp70* overexpression on the other hand showed little effects (Figure S5). All together, these findings indicate that the extent of muscle aging is interconnected with the life span of the organism.

FOXO/4E-BP Signaling in Muscles Influences Feeding Behavior and the Release of Insulin from Producing Cells

Considering that both fasting and FOXO induce *4E-BP* expression (Figure 2H), we wondered whether the systemic effect of FOXO signaling on life span extension can result, at least in part, from reduced food intake.

To test this hypothesis, we examined whether feeding behavior would be decreased in adults with FOXO and 4E-BP activation in muscles. We first monitored the amount of liquid food ingested using the CAFÉ assay (capillary feeding) (Ja et al., 2007). Interestingly, feeding was decreased in response to FOXO/4E-BP signaling in muscles (Figure 5A). To substantiate this finding, we measured the ingestion of blue-colored food (Xu et al., 2008). Also, we detected significant differences in food intake with this assay (Figure 5B), confirming
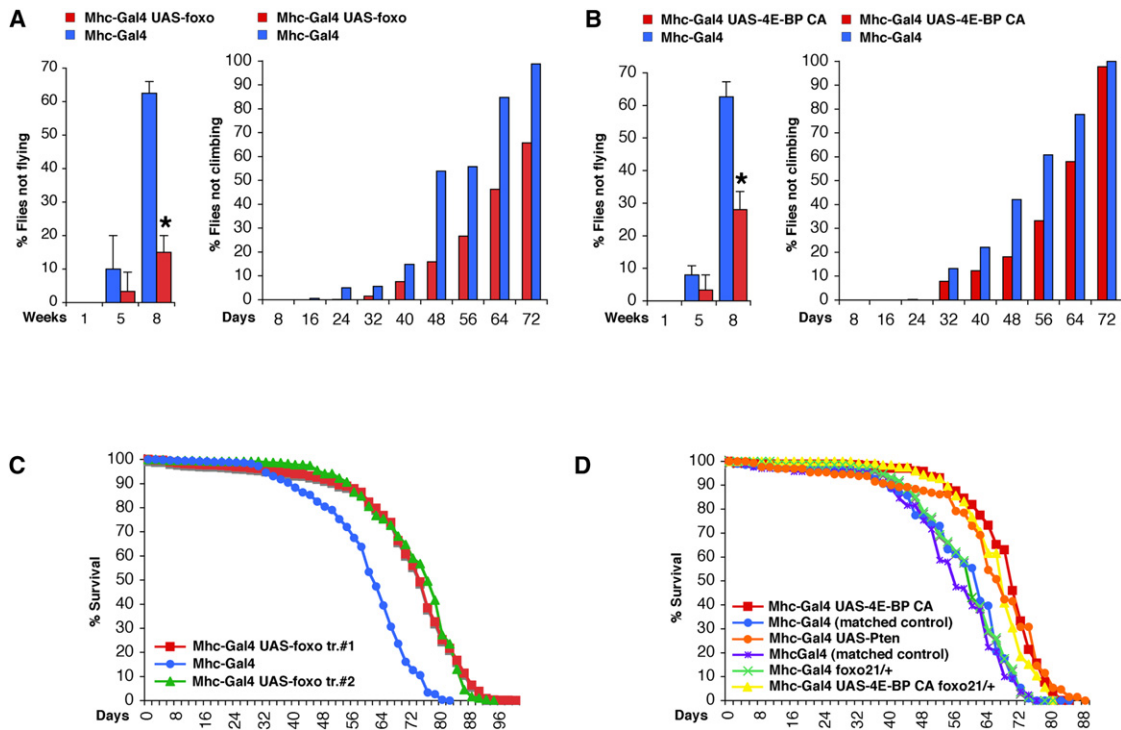
Cell

Cell
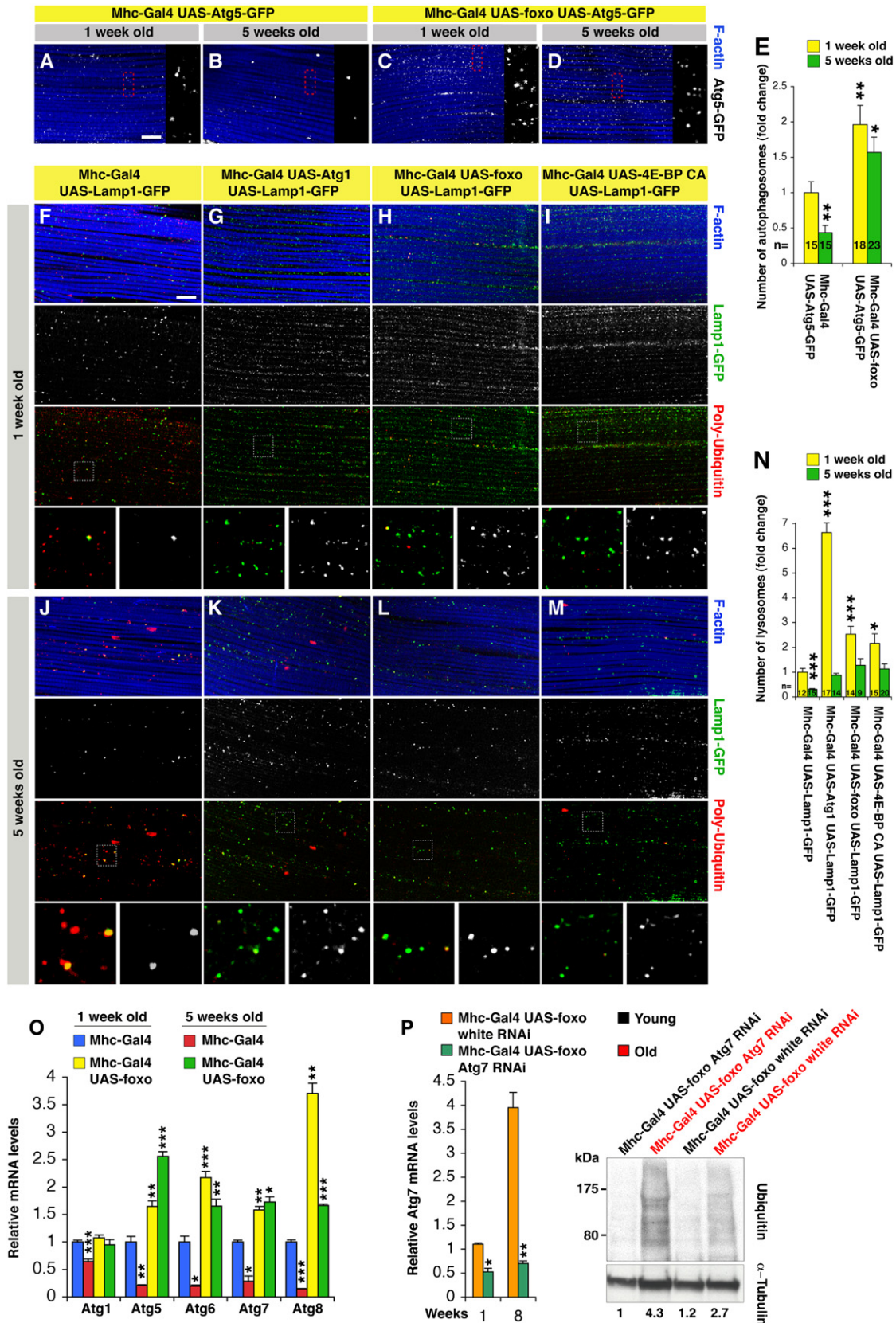
Figure 4. FOXO/4E-BP Signaling Preserves Muscle Function and Extends Life Span

(A) Muscle function gradually decreases during aging as indicated by an increase in the percentage of flies with climbing and flight defects. However, *foxo* preserves their function in comparison with controls (flight ability: n[flies] = 10 (week 1 and 5) and 30 (week 8) with n[batch] = 3 (week 1 and 5) and 2 (week 8); standard deviation (SD) is indicated and *p < 0.05. Climbing ability: (n[*Mhc-Gal4/+*] = 1264, n[*Mhc-Gal4/UAS-foxo*] = 966, with n indicating the number of flies at day 1; p < 0.001).

(B) Similar to FOXO, 4E-BP activity also results in decreased age-related flight and climbing deficits in comparison with controls (flight ability: n[flies] ≥ 10 (week 1 and 5) and 25 (week 8) with n[batch] ≥ 3 (week 1 and 5) and 2 (week 8); SD is indicated and *p < 0.05. Climbing ability: (n[*Mhc-Gal4/+*] = 204, n[*Mhc-Gal4/UAS-4E-BP CA*] = 403, p < 0.001).

(C) Survival of flies during aging. *Foxo* overexpression in muscles significantly extends the median and maximum life span (median and maximum life span: *Mhc-Gal4/+* = ∼61 and 82 days (n = 1264); *UAS-foxo tr.#1/+;Mhc-Gal4/+* = ∼73 and 100 days (n = 1184); *Mhc-Gal4/UAS-foxo tr.#2* = ∼76 and 94 days (n = 966); p < 0.001).

(D) Life span of flies with increased Pten and 4E-BP activity in muscles is extended in comparison with matched controls (median and maximum life span of 4E-BP: *Mhc-Gal4/+* = ∼63 and 78 days (n = 204); *Mhc-Gal4/UAS-4E-BP CA* = ∼71 and 84 days (n = 403); Pten: *Mhc-Gal4/+* = ∼55 and 76 days (n = 162); *Mhc-Gal4/UAS-Pten* = ∼66 and 88 days (n = 130); p < 0.001). Similar increase in life span is brought about by *4E-BP CA* overexpression in *foxo*[21] heterozygous null flies.

See also Figure S5 and Figure S7.

that feeding behavior is affected. Next, to assess whether decreased feeding behavior arises from developmental defects, we measured the body weight of adult flies, which is a sensitive indicator of developmental feeding (Demontis and Perrimon, 2009), but found no significant differences (Figure 5C). Thus, the behavior of flies overexpressing *foxo* and *4E-BP CA* in muscles most likely is not caused by developmental defects. To assess the metabolic status, we monitored the glucose concentration (glycemia) in the hemolymph. Similar to wild-type flies starved for 24 hr, we detected a significant decrease

Figure 3. FOXO and 4E-BP Regulate Proteostasis at Least in Part via the Autophagy/Lysosome System

(A–E) Immunostaining of muscles expressing the marker of autophagosomes Atg5-GFP reveals a significant increase in their number (E) and maintenance at 1 and 5 weeks of age upon *foxo* overexpression (C and D) in comparison with controls (A and B). In (E), SEM is indicated with n; *p < 0.05 and **p < 0.01.

(F–N) Immunostaining of muscles expressing the lysosomal marker Lamp1-GFP and overexpressing either *Atg1*, *foxo*, and *4E-BP CA*. Note an increase in the number of lysosomes (N) at both 1 (G-I) and 5 weeks of age (K–M), which inversely correlates with polyubiquitin immunoreactivity in comparison with control muscles (F and J). Scale bar is 10 μm (A–D and F-–M). In (N), SEM is indicated with n; *p < 0.05 and ***p < 0.001.

(O) Relative mRNA levels of autophagy genes from thoraces of 1- and 5-week-old flies decrease during normal muscle aging, while their expression increases and persists in response to FOXO. SEM is indicated with n = 4; *p,0.05, **p < 0.01 and ***p < 0.001.

(P) RNAi treatment against Atg7 results in a ∼50% knockdown of its mRNA levels in muscles and partially impairs FOXO-mediated proteostasis, as indicated by the increased detection of ubiquitin-conjugated proteins in Triton X-100 insoluble fractions at 8 weeks (old, red) in comparison with mock-treated (white RNAi) and young flies (1 week old, black). Normalized values based on α-tubulin levels are indicated.
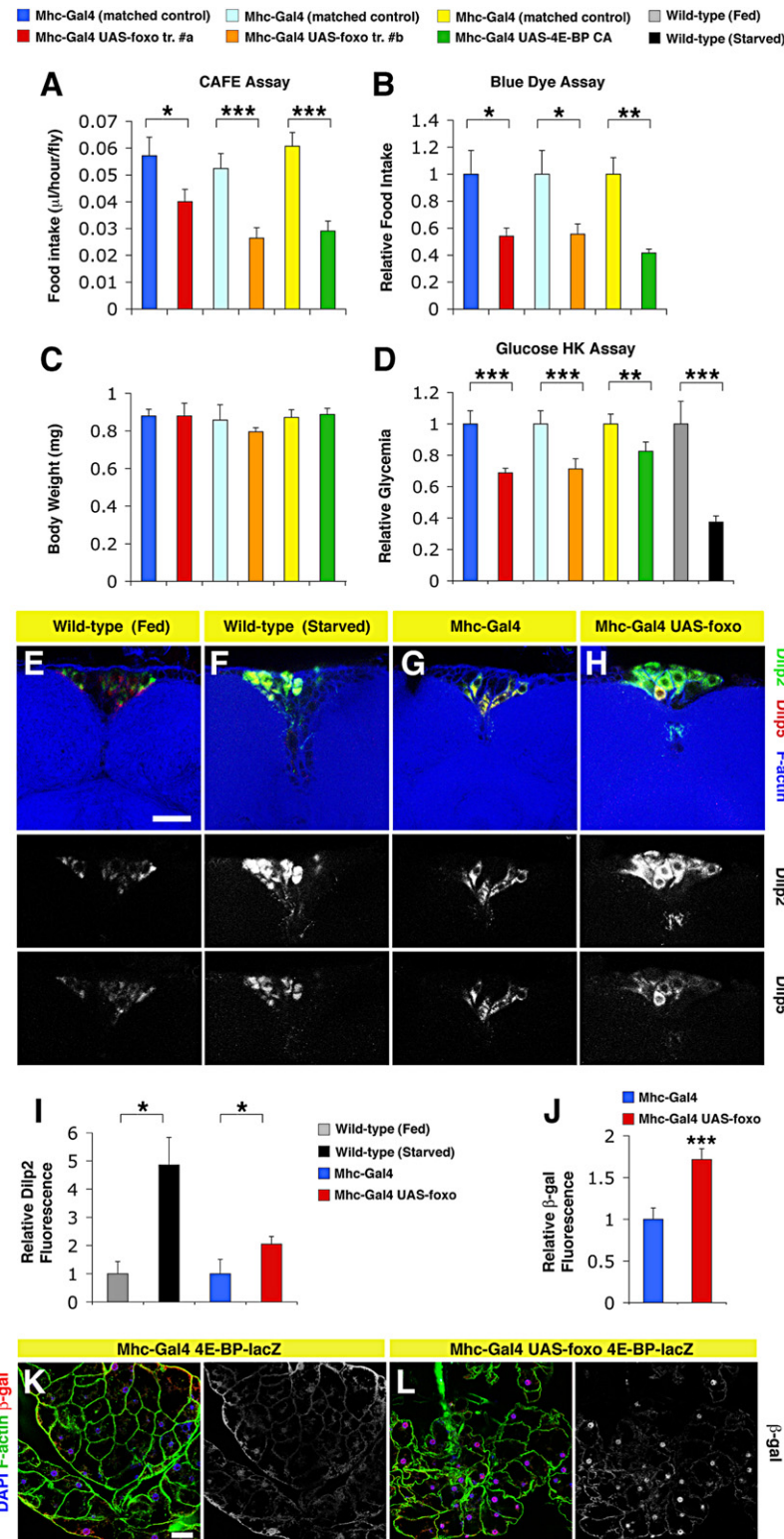
Cell

Figure 5. FOXO Signaling in Muscles Partially Mimics Systemic Metabolic Changes Associated with Fasting by Modulating Feeding Behavior

(A–C) Flies in which FOXO/4E-BP activity has been altered specifically in muscles consume less food than matched controls. Food consumption was determined via capillary feeding CAFÉ assay over 2 hr periods (A), and by monitoring the ingestion of blue colored food in 24 hr (B). Error bars represent SEM with n[measurements] = 44, 46, 52, 37, 103, and 61 in (A) and n = 2 in (B), with *p < 0.05, **p < 0.01, ***p < 0.001. Decreased feeding does not result from developmental defects, as indicated by similar body weights of flies analyzed (C) (error bars represent SD with n ≥ 3).

(D) Relative glucose levels (glycemia) in the hemolymph of flies overexpressing either *foxo* or *4E-BP CA* in muscles, and matched controls. Manipulation of FOXO/4E-BP signaling in muscles brings about a reduction of glycemia similar in part to that of wild-type flies starved for 24 hr, as estimated with the glucose hexokinase assay (SEM is indicated with n = 5, and **p < 0.01, ***p < 0.001).

(E–H) Immunostaining of Dilp-producing median neurosecretory cells in the brain of starved wild-type flies, flies overexpressing *foxo* in muscles, and controls. Increase in the immunoreactivity of insulin-like peptides Dilp2 (green) is detected in producing cells in response to either starvation (F) or *foxo* overexpression in muscles (H), in comparison respectively with fed wild-type flies (E) and controls with no *foxo* overexpression in muscles (G). Smaller changes in Dilp5 levels are observed. Phalloidin staining (blue) detects F-actin (scale bar is 20 μm; images in [E]–[H] have the same magnification).

(I) Quantification of the intensity of staining indicates that differences in Dilp2 fluorescence are significant (SD is indicated with n[measurements] = 35, 69, 37, and 96 from n[brains] = 2, 4, 3, and 4; *p < 0.05).

(J–L) Quantification and immunostaining of adipose tissue (peripheral fat body of the abdomen) from 2 week old flies. (J) Note a significant increase in nuclear β-galactosidase immunoreactivity (red) in the adipose tissue from flies with a nuclear *4E-BP-lacZ* reporter and *foxo* overexpression in muscles (L) in comparison with controls (K). F-actin (green) and DAPI staining (indicative of nuclei, blue) are shown. Scale bar is 20 μm. In (J), SEM is indicated with n = 20 and ***p < 0.001.

feeding behavior, mimic at least in part the physiological changes that are associated with fasting.

To gain mechanistic insights into the systemic regulation of aging by FOXO/4E-BP signaling in muscles, we next monitored the release of insulin-like peptides (Dilps) from the Dilp-producing median neurosecretory cells in the brain, which have been previously shown to mediate the response of life span to nutrition in *Drosophila* (Broughton et al., 2010). We detected a significant accumulation of the insulin-like peptide Dilp2 (and to a lesser extent,

of glycemia in flies with FOXO and 4E-BP activation in muscles (Figure 5D). All together, these findings suggest that FOXO and 4E-BP act as a metabolic brake in muscles that, by influencing

Dilp5) in starved wild-type flies in comparison with fed flies (Figures 5E and 5F). Increased immunoreactivity indicates decreased release of Dilps and has been previously shown to

Cell

occur in response to starvation (Geminard et al., 2009). Next, we tested whether similar changes would occur upon FOXO signaling in muscles and found a partial accumulation of Dilps (Figures 5G–5I).

Assuming that decreased Dilps secretion may result in systemic FOXO activation, we monitored its activity using a nuclear *4E-BP-lacZ* transcriptional reporter. By immunostaining adipose tissues with anti-β-galactosidase antibodies, we detected higher *4E-BP* expression upon *foxo* activation in muscles in comparison with controls (Figures 5J–5L). Thus, FOXO signaling in muscles appears to systemically activate *4E-BP* expression in other tissues by regulating food intake and insulin release.

FOXO/4E-BP Signaling in Muscles Regulates Proteostasis in Other Aging Tissues

Our demonstration that FOXO/4E-BP signaling in muscles extends life span in *Drosophila* and induces a systemic fasting-like response, along with the observation that muscles undergo age-related structural and functional changes precociously in comparison with other tissues (Herndon et al., 2002; Zheng et al., 2005), raises the possibility that muscle senescence may influence the progression of age-related degenerative events in the entire organism.

To test this hypothesis, we examined whether, in addition to life span extension, FOXO signaling in muscles can affect protein homeostasis in other tissues. As in the case of muscles (Figure 1 and Figure 2), we found that Ref(2)P/polyubiquitin aggregates progressively accumulate in aging retinas (Figures 6A and 6D), brains (Figures 6B and 6E), and adipose tissue (Figures 6C and 6F) (peripheral fat body of the abdomen). However, *foxo* overexpression in muscle resulted in decreased accumulation of protein aggregates in other aging tissues (Figures 6D–6F; quantification in Figure 6G). Similar changes were observed in response to 4E-BP activity in muscles in comparison with syngenic controls (Figure 6H). Importantly, this regulation is muscle nonautonomous, as Mhc-Gal4 drives transgene expression only in muscles (and not in the retina, brain or adipose tissue) (Figure S1). To further test the finding that FOXO/4E-BP signaling in muscles delays the systemic impairment of proteostasis in other tissues (Figures 6A–6H), we analyzed by western blot the ubiquitin levels of Triton X-100 insoluble fractions, which included protein aggregates, from either thoraces (which mainly consist of *foxo*-overexpressing muscles) or heads and abdomens (which are enriched in nonmuscle tissues and muscles with little *foxo* overexpression) (Figure S1), at 1 and 8 weeks of age. In agreement with the increased deposition of protein aggregates observed during aging by immunofluorescence (Figure 1, Figure 2, and Figures 6A–6F), ubiquitin levels were dramatically increased in the Triton X-100 insoluble fractions from control thoraces, and head and abdominal extracts at 8 weeks of age, in comparison with 1 week of age (Figure 6I). However, ubiquitin levels were only partially increased in old *foxo*-overexpressing flies in both thoracic and head and abdominal extracts. No substantial differences were instead detected in the Triton X-100 soluble fractions (data not shown). Similar results were obtained by *4E-BP CA* but not *Hsp70* overexpression in muscles (Figure 6I; Figure S5), indicating that 4E-BP

activity in muscles also confers systemic protection from the age-related decline in proteostasis. To test whether this effect is muscle-specific, we overexpressed *foxo* in the adipose tissue (abdominal fat body) with the S106GS-Gal4 driver, and analyzed the deposition of polyubiquitinated proteins in Triton X-100 insoluble fractions from thoraces. Under these conditions, we seemingly detected no differences (Figure S6), suggesting that, although other tissues may be involved, muscles may play a key role in this regulation. Altogether, these observations suggest that FOXO and 4E-BP activity in muscles mitigates the loss of proteostasis nonautonomously by influencing feeding behavior, insulin release from producing cells, and 4E-BP activity in other tissues.

DISCUSSION

By using a number of behavioral, genetic, and molecular assays, we have described a mechanism in the pathogenesis of muscle aging that is based on the loss of protein homeostasis (proteostasis) and the resulting decrease in muscle strength (Figure 7). Increased activity of Pten and the transcription factor FOXO is sufficient to delay this process, while *foxo* null animals experience accelerated loss of proteostasis during muscle aging. Pten and FOXO induce multiple protective responses, including the expression of folding chaperones and the regulator of protein translation 4E-BP that has a pivotal role in preserving proteostasis. FOXO and 4E-BP preserve muscle function, at least in part by sustaining the basal activity of the autophagy/lysosome system, which removes aggregates of damaged proteins. However, additional mechanisms may be involved. For example, the proteasome system may degrade damaged proteins and thus avoid their accumulation in aggregates (Rubinsztein, 2006). Thus, perturbation in proteasome assembly and subunit composition may contribute to muscle aging in response to FOXO activity. In addition, whereas overexpression of a single chaperone had limited effects, interventions to effectively limit the extent of protein damage are likely to delay the decay in proteostasis by decreasing the workload for the proteasome and autophagy systems (Tower, 2009).

By comparing the accumulation of polyubiquitinated proteins in aggregates of aging muscles, retinas, brains, and adipose tissue, we have found that reduced protein homeostasis is a general feature of tissue aging that is particularly prominent in muscles (Figure 1, Figure 6, and Figure S6). The observation that muscle aging is characterized by loss of proteostasis further suggests some similarity between muscle aging and neurodegenerative diseases, many of which are characterized by the accumulation of protein aggregates (Rubinsztein, 2006).

Mechanical, thermal, and oxidative stressors occur during muscle contraction (Arndt et al., 2010), and therefore muscle proteins may be particularly susceptible to damage in comparison with other tissues. While our findings refer to the loss of proteostasis in the context of normal aging, it is likely that a better understanding of this process will help cure muscle pathologies associated with aging, as some of the underlying mechanisms of etiology may be shared. For example, most cases of inclusion body myositis (IBM) arise over the age of 50 years, defining aging as a major risk factor for the pathogenesis of this disease.
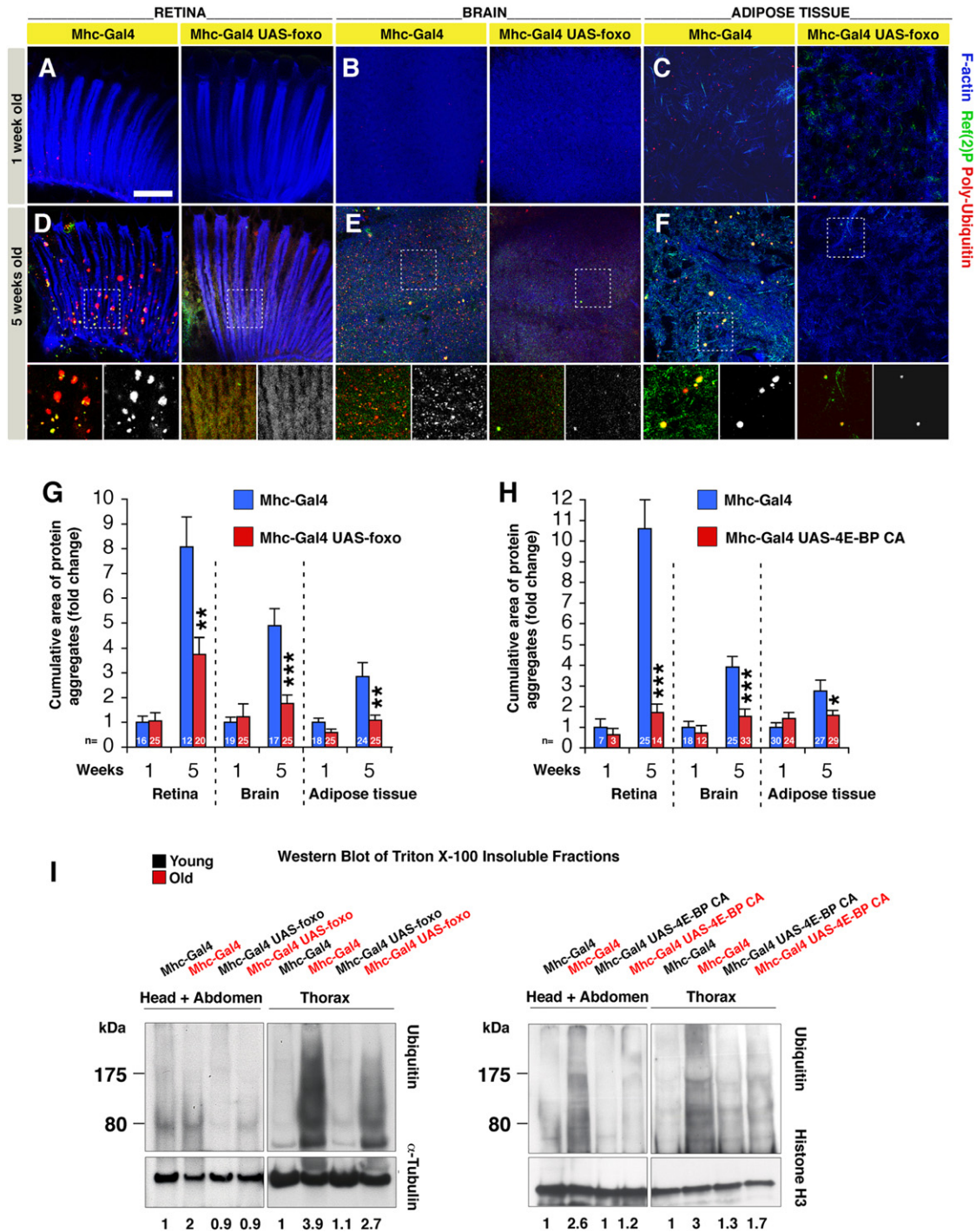
Cell

Figure 6. Systemic Proteostasis is Remotely Controlled by FOXO/4E-BP Signaling in Muscles

(A–F) Aggregates of polyubiquitin proteins accumulate during aging in the retina (A and D), brain (B and E), and the adipose tissue (C and F) of control flies (*Mhc-Gal4/+*), but to a lesser extent in tissues from flies overexpressing *foxo* in muscles (*UAS-foxo/+;Mhc-Gal4/+*), as indicated by polyubiquitin (red) and p62/Ref(2)P (green) stainings. Phalloidin staining (blue) outlines F-actin. Note that Mhc-Gal4 does not drive transgene expression in these tissues (Figure S1). Scale bar is 10 μm.

(G and H) The age-related increase in the cumulative area of protein aggregates is significantly less prominent in tissues from flies overexpressing *foxo* (G) or *4E-BP CA* (H) in muscles in comparison with controls (SEM is indicated with n; *p < 0.05. **p < 0.01, and ***p < 0.001).

(I) Ubiquitin levels (indicative of protein aggregates) are detected in Triton X-100 insoluble fractions from thoraces, and head and abdominal tissues from flies overexpressing *foxo* in muscles or control flies at 1 (young, black) and 8 (old, red) weeks of age. Ubiquitin levels are increased in old flies in comparison with young
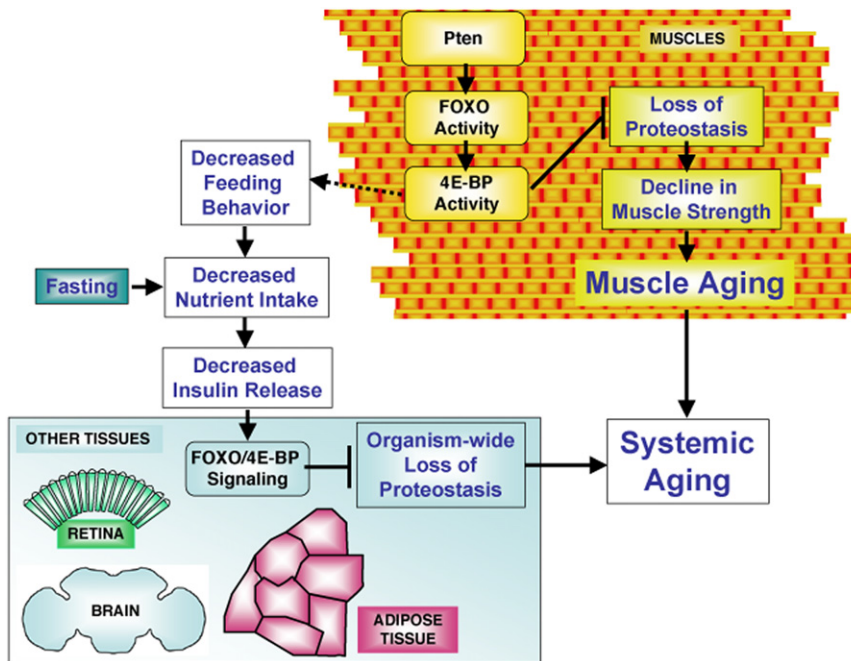
Cell

Figure 7. FOXO/4E-BP Signaling in Muscles Controls Proteostasis and Systemic Aging
Muscle aging is characterized by protein damage and accumulation of cytoplasmic aggregates. Loss of protein homeostasis (proteostasis) associates with the progressive decrease in muscle strength and can affect the life span of the organism. Pten/FOXO signaling induces multiple targets including several folding chaperones and the regulator of protein translation 4E-BP. FOXO/4E-BP activity regulates muscle proteostasis at least in part via the autophagy/lysosome pathway of protein degradation, preserves muscle function, and extends life span. In addition, FOXO/4E-BP signaling in muscles decreases feeding behavior that, similar to fasting, results in reduced insulin release from producing cells. This in turn promotes FOXO and 4E-BP activity in other tissues, preserving proteostasis organism-wide and mitigating systemic aging.

Interestingly, muscle weakness in patients with IBM is characterized by the accumulation of protein aggregates (Needham and Mastaglia, 2008), which we have now described as occurring in the context of regular muscle aging in *Drosophila*. Thus, FOXO may interfere with the pathogenesis of muscle degenerative diseases in addition to muscle aging. Studies in animal disease models of IBM will be needed to test this hypothesis.

There is an apparent contradiction between our findings and the data describing the FOXO-dependent induction of muscle atrophy in mice (Bodine et al., 2001; Sandri et al., 2004), a serious form of age-related muscle degeneration that results in decreased muscle strength (Augustin and Partridge, 2009). The observation that different degrees of FOXO activation can promote stress resistance, or rather cell death (Salih and Brunet, 2008), could explain why FOXO activity can be protective or rather detrimental during muscle aging. In particular, while physiologic FOXO activation can preserve protein homeostasis and muscle function, its excessive activation may lead to decreased muscle function due to hyperactivation of the protein turnover pathways. Consistent with this view, the macroautophagy pathway has also been involved in both muscle atrophy (Mammucari et al., 2007; Zhao et al., 2007) and in the preservation of muscle sarcomere organization (Arndt et al., 2010; Masiero et al., 2009), highlighting the importance of fine-tuning the degree of activation of stress resistance pathways to maintain muscle homeostasis. In addition, the output of FOXO activity may radically differ in growing versus preexisting myofibers. In particular, our present study indicates that FOXO protects

preexisting myofibers against age-dependent changes in proteostasis while also blunting developmental muscle growth in flies (Demontis and Perrimon, 2009), as observed in mammals (Kamei et al., 2004). Thus, deleterious effects of FOXO activation as observed in mammalian muscles may result from the inhibition of the growth of novel myofibers in postnatal development and adulthood, a process which is thought to be limited to development in *Drosophila* (Grefte et al., 2007).

An interesting observation of our study is that interventions that decrease muscle aging also extend the life span of the organism. In particular, our work raises the prospect that the extent of muscle aging may be a key determinant of systemic aging (Figure 7). Reduced muscle proteostasis may be detrimental per se for life expectancy, presumably due to the involvement of muscles in a number of key physiological functions. Consistent with this view, overexpression in muscles of aggregation-prone human Huntington's disease proteins is sufficient to decrease life span (Figure S7). Moreover, FOXO signaling in muscles regulates proteostasis in other tissues, via the inhibition of feeding behavior and the decreased release of insulin from producing cells, which in turn promote 4E-BP activity systemically. Thus, we propose that FOXO/4E-BP signaling in muscles regulate life span and remotely control aging events in other tissues by bringing about some of the protection associated with decreased food intake.

In mammals, muscles produce a number of cytokines involved in the control of systemic metabolism (Nair, 2005; Pedersen and Febbraio, 2008). For example, interleukin-6 (IL-6) is produced by muscles and has been proposed to control glucose homeostasis and feeding behavior through peripheral and brain mechanisms (Febbraio and Pedersen, 2002; Plata-Salaman, 1998). Thus,

flies in extracts from both muscles (thoraces) and nonmuscle tissues (heads and abdomens). However, flies overexpressing *foxo* in muscles have reduced deposition of protein aggregates at 8 weeks of age in both muscles and nonmuscle tissues. Similar results are obtained in response to increased 4E-BP activity in muscles (l), but not Hsp70 (Figure S5). Quantification of ubiquitin-conjugated proteins normalized to α-tubulin or histone H3 levels is indicated. See also Figures S1, Figure S5, and Figure S6.

a muscle-based network of systemic aging as observed in flies may occur in humans.

This study supports the common belief that preserving muscle function is beneficial for overall aging (Boyle et al., 2009; Chen et al., 2005), and the notion that muscles are central tissues to coordinate organism-wide processes, including aging and metabolic homeostasis (Nair, 2005). Moreover, the observation that FOXO signaling in muscles influences aging events in other tissues suggests that the systemic regulation of aging relies on tissue-to-tissue communication (Russell and Kahn, 2007), which may provide the basis for interventions to extend healthy life span.

EXPERIMENTAL PROCEDURES

Drosophila Strains and Life Span Analysis
Details on fly strains can be found in Extended Experimental Procedures.

For longevity measurement, male flies were collected within 24 hr from eclosion and reared at standard density (20 flies per vial) on cornmeal/soy flour/yeast fly food at 25°C. Dead flies were counted every other day and food changed. For each genotype, at least two independent cohorts of flies, raised at different times from independent crosses, were analyzed. For starvation treatments, flies were kept in normal vials with 1.5% agar as a water source for the period of time indicated. For all experiments, Mhc-Gal4 females were mated with male transgenic and syngenic control flies, and the resulting male offspring analyzed in parallel by comparing transgene expressing flies with matched controls flies having the same genetic background. For transgene expression with the Gal4-UAS system, flies were reared at 25°C.

Behavioral and Metabolic Assays
Flight ability was scored according to Park et al. (2006), and negative geotaxis assays were performed as previously described (Rhodenizer et al., 2008). In brief, flies were gently tapped to the bottom of a plastic vial, and the number of flies that could climb to the top of the vial after 20 s was scored. Quantification of the glucose concentration in the hemolymph, and capillary (CAFÉ) and blue-colored food feeding assays were done as previously described (Geminard et al., 2009; Xu et al., 2008) and are described in detail in Extended Experimental Procedures.

Immunostaining, Confocal and Electron Microscopy, and Image Analysis
For whole-mount immunostaining of the fly tissues, indirect flight muscles, and peripheral fat body of the abdomen, retinas, and brains were dissected from male flies and fixed for 30–40 min in PBS with 4% paraformaldehyde and 0.2% Triton X-100. After washing, samples were incubated overnight with appropriate primary and secondary antibodies. Image analysis was done with ImageJ and Photoshop. Immuno-gold electron microscopy was done similar to Nezis et al., (2008). See Extended Experimental Procedures for further information and a list of the antibodies used.

Quantitative Real-Time RT-PCR
qRT-PCR was done as previously described (Demontis and Perrimon, 2009). Total RNA was prepared from fly thoraces and qRT-PCR was performed with the QuantiTect SYBR Green PCR kit (QIAGEN). *Alpha-Tubulin 84B* that was used has normalization reference. Relative quantification of mRNA levels was calculated using the comparative C_T method.

Statistical Analysis
Statistical analysis was performed with Excel (Microsoft) and p values were calculated with Student's t tests and log-rank tests.

Western Blot and Biochemical Analysis of Detergent-Insoluble Fractions
Western blot and biochemical analysis of detergent-insoluble fractions were done substantially as previously described (Nezis et al., 2008). In brief, dissected flies were homogenized in ice-cold PBS with 1% Triton X-100 and protease inhibitors, and the resulting unsoluble pellet resuspended in RIPA buffer with 5% SDS and 8M urea. See Extended Experimental Procedures for a complete protocol.

SUPPLEMENTAL INFORMATION

Supplemental Information includes Extended Experimental Procedures, seven figures, and two tables and can be found with this article online at doi:10.1016/j.cell.2010.10.007.

REFERENCES

Arndt, V., Dick, N., Tawo, R., Dreiseidler, M., Wenzel, D., Hesse, M., Furst, D.O., Saftig, P., Saint, R., Fleischmann, B.K., et al. (2010). Chaperone-assisted selective autophagy is essential for muscle maintenance. Curr. Biol. *20*, 143–148.

Augustin, H., and Partridge, L. (2009). Invertebrate models of sge-telated muscle fegeneration. Biochim. Biophys. Acta *1790*, 1084–1094.

Bodine, S.C., Stitt, T.N., Gonzalez, M., Kline, W.O., Stover, G.L., Bauerlein, R., Zlotchenko, E., Scrimgeour, A., Lawrence, J.C., Glass, D.J., and Yancopoulos, G.D. (2001). Akt/mTOR pathway is a crucial regulator of skeletal muscle hypertrophy and can prevent muscle atrophy in vivo. Nat. Cell Biol. *3*, 1014–1019.

Boyle, P.A., Buchman, A.S., Wilson, R.S., Leurgans, S.E., and Bennett, D.A. (2009). Association of muscle strength with the risk of Alzheimer disease and the rate of cognitive decline in community-dwelling older persons. Arch. Neurol. *66*, 1339–1344.

Broughton, S.J., Slack, C., Alic, N., Metaxakis, A., Bass, T.M., Driege, Y., and Partridge, L. (2010). DILP-producing median neurosecretory cells in the *Drosophila* brain mediate the response of lifespan to nutrition. Aging Cell *9*, 336–346.

Chen, H., Zhang, S.M., Schwarzschild, M.A., Hernan, M.A., and Ascherio, A. (2005). Physical activity and the risk of Parkinson disease. Neurology *64*, 664–669.

Cohen, E., Bieschke, J., Percivalle, R.M., Kelly, J.W., and Dillin, A. (2006). Opposing activities protect against age-onset proteotoxicity. Science *313*, 1604–1610.

Demontis, F., and Perrimon, N. (2009). Integration of Insulin receptor/Foxo signaling and dMyc activity during muscle growth regulates body size in *Drosophila*. Development *136*, 983–993.

Febbraio, M.A., and Pedersen, B.K. (2002). Muscle-derived interleukin-6: mechanisms for activation and possible biological roles. FASEB J. *16*, 1335–1347.

Garigan, D., Hsu, A.L., Fraser, A.G., Kamath, R.S., Ahringer, J., and Kenyon, C. (2002). Genetic analysis of tissue aging in Caenorhabditis elegans: a role for heat-shock factor and bacterial proliferation. Genetics *161*, 1101–1112.

Geminard, C., Rulifson, E.J., and Leopold, P. (2009). Remote control of insulin secretion by fat cells in *Drosophila*. Cell Metab. *10*, 199–207.

Giannakou, M.E., Goss, M., Junger, M.A., Hafen, E., Leevers, S.J., and Partridge, L. (2004). Long-lived *Drosophila* with overexpressed dFOXO in adult fat body. Science *305*, 361.

Gorski, S.M., Chittaranjan, S., Pleasance, E.D., Freeman, J.D., Anderson, C.L., Varhol, R.J., Coughlin, S.M., Zuyderduyn, S.D., Jones, S.J., and Marra, M.A. (2003). A SAGE approach to discovery of genes involved in autophagic cell death. Curr. Biol. *13*, 358–363.

Grefte, S., Kuijpers-Jagtman, A.M., Torensma, R., and Von den Hoff, J.W. (2007). Skeletal muscle development and regeneration. Stem Cells Dev. *16*, 857–868.

Hara, T., Nakamura, K., Matsui, M., Yamamoto, A., Nakahara, Y., Suzuki-Migishima, R., Yokoyama, M., Mishima, K., Saito, I., Okano, H., and Mizushima, N. (2006). Suppression of basal autophagy in neural cells causes neurodegenerative disease in mice. Nature *441*, 885–889.

Herndon, L.A., Schmeissner, P.J., Dudaronek, J.M., Brown, P.A., Listner, K.M., Sakano, Y., Paupard, M.C., Hall, D.H., and Driscoll, M. (2002). Stochastic and genetic factors influence tissue-specific decline in ageing *C. elegans*. Nature *419*, 808–814.

Hsu, A.L., Murphy, C.T., and Kenyon, C. (2003). Regulation of aging and age-related disease by DAF-16 and heat-shock factor. Science *300*, 1142–1145.

Hwangbo, D.S., Gershman, B., Tu, M.P., Palmer, M., and Tatar, M. (2004). *Drosophila* dFOXO controls lifespan and regulates insulin signalling in brain and fat body. Nature *429*, 562–566.

Ja, W.W., Carvalho, G.B., Mak, E.M., de la Rosa, N.N., Fang, A.Y., Liong, J.C., Brummel, T., and Benzer, S. (2007). Prandiology of *Drosophila* and the CAFE assay. Proc. Natl. Acad. Sci. USA *104*, 8253–8256.

Junger, M.A., Rintelen, F., Stocker, H., Wasserman, J.D., Vegh, M., Radimerski, T., Greenberg, M.E., and Hafen, E. (2003). The *Drosophila* forkhead transcription factor FOXO mediates the reduction in cell number associated with reduced insulin signaling. J. Biol. *2*, 20.

Kamei, Y., Miura, S., Suzuki, M., Kai, Y., Mizukami, J., Taniguchi, T., Mochida, K., Hata, T., Matsuda, J., Aburatani, H., et al. (2004). Skeletal muscle FOXO1 (FKHR) transgenic mice have less skeletal muscle mass, down-regulated Type I (slow twitch/red muscle) fiber genes, and impaired glycemic control. J. Biol. Chem. *279*, 41114–41123.

Kenyon, C. (2005). The plasticity of aging: insights from long-lived mutants. Cell *120*, 449–460.

Korolchuk, V.I., Mansilla, A., Menzies, F.M., and Rubinsztein, D.C. (2009). Autophagy inhibition compromises degradation of ubiquitin-proteasome pathway substrates. Mol. Cell *33*, 517–527.

Libina, N., Berman, J.R., and Kenyon, C. (2003). Tissue-specific activities of *C. elegans* DAF-16 in the regulation of lifespan. Cell *115*, 489–502.

Mammucari, C., Milan, G., Romanello, V., Masiero, E., Rudolf, R., Del Piccolo, P., Burden, S.J., Di Lisi, R., Sandri, C., Zhao, J., et al. (2007). FoxO3 controls autophagy in skeletal muscle in vivo. Cell Metab. *6*, 458–471.

Masiero, E., Agatea, L., Mammucari, C., Blaauw, B., Loro, E., Komatsu, M., Metzger, D., Reggiani, C., Schiaffino, S., and Sandri, M. (2009). Autophagy is required to maintain muscle mass. Cell Metab. *10*, 507–515.

Morley, J.F., Brignull, H.R., Weyers, J.J., and Morimoto, R.I. (2002). The threshold for polyglutamine-expansion protein aggregation and cellular toxicity is dynamic and influenced by aging in *Caenorhabditis elegans*. Proc. Natl. Acad. Sci. USA *99*, 10417–10422.

Nair, K.S. (2005). Aging muscle. Am. J. Clin. Nutr. *81*, 953–963.

Needham, M., and Mastaglia, F.L. (2008). Sporadic inclusion body myositis: a continuing puzzle. Neuromuscul. Disord. *18*, 6–16.

Nezis, I.P., Simonsen, A., Sagona, A.P., Finley, K., Gaumer, S., Contamine, D., Rusten, T.E., Stenmark, H., and Brech, A. (2008). Ref(2)P, the *Drosophila* melanogaster homologue of mammalian p62, is required for the formation of protein aggregates in adult brain. J. Cell Biol. *180*, 1065–1071.

Park, J., Lee, S.B., Lee, S., Kim, Y., Song, S., Kim, S., Bae, E., Kim, J., Shong, M., Kim, J.M., and Chung, J. (2006). Mitochondrial dysfunction in *Drosophila* PINK1 mutants is complemented by parkin. Nature *441*, 1157–1161.

Pedersen, B.K., and Febbraio, M.A. (2008). Muscle as an endocrine organ: focus on muscle-derived interleukin-6. Physiol. Rev. *88*, 1379–1406.

Plata-Salaman, C.R. (1998). Cytokines and feeding. News Physiol. Sci. *13*, 298–304.

Rhodenizer, D., Martin, I., Bhandari, P., Pletcher, S.D., and Grotewiel, M. (2008). Genetic and environmental factors impact age-related impairment of negative geotaxis in *Drosophila* by altering age-dependent climbing speed. Exp. Gerontol. *43*, 739–748.

Rubinsztein, D.C. (2006). The roles of intracellular protein-degradation pathways in neurodegeneration. Nature *443*, 780–786.

Russell, S.J., and Kahn, C.R. (2007). Endocrine regulation of ageing. Nat. Rev. Mol. Cell Biol. *8*, 681–691.

Rusten, T.E., Lindmo, K., Juhasz, G., Sass, M., Seglen, P.O., Brech, A., and Stenmark, H. (2004). Programmed autophagy in the *Drosophila* fat body is induced by ecdysone through regulation of the PI3K pathway. Dev. Cell *7*, 179–192.

Salih, D.A., and Brunet, A. (2008). FoxO transcription factors in the maintenance of cellular homeostasis during aging. Curr. Opin. Cell Biol. *20*, 126–136.

Sandri, M., Sandri, C., Gilbert, A., Skurk, C., Calabria, E., Picard, A., Walsh, K., Schiaffino, S., Lecker, S.H., and Goldberg, A.L. (2004). Foxo transcription factors induce the atrophy-related ubiquitin ligase atrogin-1 and cause skeletal muscle atrophy. Cell *117*, 399–412.

Simonsen, A., Cumming, R.C., Brech, A., Isakson, P., Schubert, D.R., and Finley, K.D. (2008). Promoting basal levels of autophagy in the nervous system enhances longevity and oxidant resistance in adult *Drosophila*. Autophagy *4*, 176–184.

Tain, L.S., Mortiboys, H., Tao, R.N., Ziviani, E., Bandmann, O., and Whitworth, A.J. (2009). Rapamycin activation of 4E-BP prevents parkinsonian dopaminergic neuron loss. Nat. Neurosci. *12*, 1129–1135.

Tower, J. (2009). Hsps and aging. Trends Endocrinol. Metab. *20*, 216–222.

Wang, M.C., Bohmann, D., and Jasper, H. (2005). JNK extends life span and limits growth by antagonizing cellular and organism-wide responses to insulin signaling. Cell *121*, 115–125.

Wessells, R.J., Fitzgerald, E., Cypser, J.R., Tatar, M., and Bodmer, R. (2004). Insulin regulation of heart function in aging fruit flies. Nat. Genet. *36*, 1275–1281.

Wolkow, C.A., Kimura, K.D., Lee, M.S., and Ruvkun, G. (2000). Regulation of *C. elegans* life-span by insulinlike signaling in the nervous system. Science *290*, 147–150.

Xu, K., Zheng, X., and Sehgal, A. (2008). Regulation of feeding and metabolism by neuronal and peripheral clocks in *Drosophila*. Cell Metab. *8*, 289–300.

Zhao, J., Brault, J.J., Schild, A., Cao, P., Sandri, M., Schiaffino, S., Lecker, S.H., and Goldberg, A.L. (2007). FoxO3 coordinately activates protein degradation by the autophagic/lysosomal and proteasomal pathways in atrophying muscle cells. Cell Metab. *6*, 472–483.

Zheng, J., Edelman, S.W., Tharmarajah, G., Walker, D.W., Pletcher, S.D., and Seroude, L. (2005). Differential patterns of apoptosis in response to aging in *Drosophila*. Proc. Natl. Acad. Sci. USA *102*, 12083–12088.

Zid, B.M., Rogers, A.N., Katewa, S.D., Vargas, M.A., Kolipinski, M.C., Lu, T.A., Benzer, S., and Kapahi, P. (2009). 4E-BP extends lifespan upon dietary restriction by enhancing mitochondrial activity in Drosophilia. Cell *139*, 149–160.

Supplemental Information

EXTENDED EXPERIMENTAL PROCEDURES

Fly Stocks

Fly stocks used are: *y w; UAS-foxo-TM* (constitutive active); *y w; UAS-foxo transgene #1 #a* (Hwangbo et al., 2004); *y w; UAS-foxo transgene #2*, and *y w; foxo²¹* and *y w; foxo²⁵* (Junger et al., 2003; Zheng et al., 2007); *y w, UAS-foxo transgene #b* (Puig et al., 2003); *y w, UAS-4E-BP CA* ((Miron et al., 2001); Bloomington #24854; recombined on *y w*); *4E-BP/Thor-lacZ* (Bloomington #9558); *y w; UAS-Pten* ((Huang et al., 1999); recombined on *y w*); *y w; Mhc-GFP* (WeeP26; Clyne et al., 2003); *UAS-Lamp1-GFP* (Pulipparacharuvil et al., 2005); *y w; UAS-GFP-Atg5* (Bloomington #8731; (Rusten et al., 2004)); *UAS-HD-Q72-GFP* and *UAS-HD-Q103-GFP* (gift of Sheng Zhang, University of Texas); *y w; Dmef2-Gal4* (Ranganayakulu et al., 1996); *w; UAS-srcGFP* (Bloomington #5432); *S106GS-Gal4* (Giannakou et al., 2004); and *w; Mhc-Gal4* (Schuster et al., 1996). RNAi stocks to knock-down *Atg7* (JF02787) and *white* (JF01786) mRNA levels were provided by the DRSC/TRiP at Harvard Medical School. *UAS-Hsp70* transgenic flies were generated by cloning the *Hsp70* coding sequence in the pUAST vector followed by injection into *w¹¹¹⁸* embryos.

Antibodies and Immunostaining Procedures

Antibodies used are: anti-β-galactosidase (Promega, 1:200), anti-GFP (Abcam, 1:200), anti-polyubiquitin (FK2; Assay Designs,1:200), anti-Hsp70 (1:200; gift of Susan Lindquist), anti-Ref(2)P (1:1000; gift of Ioannis Nezis (Nezis et al., 2008)), anti-Tropomyosin (Babraham Institute, 1:100), and/or anti-Dilp2 and anti-Dilp5 (Geminard et al., 2009) antibodies.

After incubation with primary antibodies over night, the samples were washed, and incubated with Alexa488 or Alexa635-conjugated phalloidin (1:100), to visualize F-actin, and with Alexa-conjugated secondary antibodies (Molecular Probes, 1:200). Nuclei were visualized by DAPI staining (1 μg/ml). Samples were processed with a Leica SP2 laser scanning confocal microscope.

Detailed Behavioral and Metabolic Assays

CAFÉ feeding behavior assays were done as previously (Ja et al., 2007; Xu et al., 2008). In brief, twelve hours before the assay, 7 flies were transferred from normal food to 1.5% agar vials and fed 5% sucrose solution maintained in 5 μl calibrated glass micropipettes (VWR, #53432-706). At the start of the assay, the old micropipette was replaced with a new one. The amount of liquid food consumed was recorded every 2 hr and corrected on the basis of the evaporation observed in a vial without flies.

Feeding assays on blue colored food were done by providing food containing 5% sucrose, 1% agar, and 0.5% brilliant blue for 24 hr. Blue dye ingestion was quantified by measuring the absorbance at 625 nm of batches of 4 flies, as done previously (Xu et al., 2008). For measurement of body weight, groups of 7 flies were weighted on a precision balance and the average body weight calculated.

The quantification of the glucose concentration in the hemolymph was done according to Geminard et al., (2009). In brief, at least 15 flies were decapitated, placed in a perforated 0.5 ml tube, centrifuged for 6 min at 1500 g, and the hemolymph collected in an underlying 1.5 ml tube at 4°C. The hemolymph was diluted 1:10 in distilled water and the glucose concentration was determined with the Glucose Hexokinase Assay kit (Sigma #GAHK-20) after trehalose conversion into glucose with porcine trehalase (Sigma #T8778) and incubation at 37°C overnight. All experiments were done with male flies.

Cell Culture and Luciferase Assays

For transcriptional assays, S2R+ cells were transfected with the following plasmids: pMT-foxo (Puig et al., 2003), actin-firefly Luciferase, and either wild-type of mutant versions of *Renilla* Luciferase reporters based on the promoters of Hsp70, Hsp40, and Hsp90. *Renilla* Luciferase reporters were constructed and mutagenized via a standard PCR-based approach. Luciferase activity refers to the ratio of *Renilla* to firefly Luciferase luminescence.

List of qPCR Primers

Alpha-Tubulin84B (CG1913):
5′-GCTGTTCCACCCCGAGCAGCTGATC-3′ and 5′-GGCGAACTCCAGCTTGGACTTCTTGC-3′
Thor/4E-BP (CG8846):
5′-TCCTGGAGGCACCAAACTTATC-3′ and 5′-GGAGCCACGGAGATTCTTCA-3′
Hsp70Bbb (CG5834):
5′-GGAGACACACACTTGGGCGGCGAG-3′ and 5′-TCTCGATGGTGGCCTCCGTGCTAG-3′
Hip (CG2947):
5′-TCCCGAGGTGTCAGCCGCCATTCAGGAC-3′ and 5′-CAAACCGTCATCGACGAAGTCGGCGGAG-3′
Hop (CG2720):
5′-AAGGCCTTCGAAGCGTACAACGAGGGTC-3′ and 5′-TCCTCTACCCGAGGTTCAGCGGGCTTTG-3′
Hsp40 (*DnaJ-like-1*, CG10578):
5′-CTACAAGATTCTGGGCCTCGAGCGC-3′ and 5′-CGTAATTGTCGAAGATGTCGCGCTTC-3′
Hsp90 (*Hsp83*, CG1242):
5′-AGAAGCAGAGACCTTTGCATTCCAG-3′ and 5′-AGCTTGATGTACAGCTCCTTGCCAG-3′
CHIP (CG5203):

5′-TTGCTACTCAAAGGCCATCATAAAG-3′ and 5′-TATGCCCGTTGAAGGTGCTTTATAG-3′
Chap1 (*CG14224*):
5′-ACGGTCGAAGTTGACGAAGATTCTGG-3′ and 5′-AAAGGGCGTTTGGCGCACGTCAG-3′
Hsc70.1 (*CG8937*):
5′-GAATCCCAACAACACGATCTTTGATG-3′ and 5′-AGGTAGGCCTCCGCGGTCTCTC-3′
Atg1 (CG10967):
5′-CGTCTACAAAGGACGTCATCGCAAGAAAC-3′ and 5′-CGCCAAGTCGCCGCCATTGCAATACTC-3′
Atg5 (CG1643):
5′-CCTGCGAATCTATACAGACGATGAC-3′ and 5′-AGCTCAGATGCTCGGACATCCATTG-3′
Atg6 (CG5429):
5′-TGCACGCAATGGCGGAGTTATCTTTGC-3′ and 5′-CAGCTCCGCTTTCAGCTTAAAAGCAGC-3′
Atg7 (CG5489):
5′-TGCCTTTCTGCTTCAGCAATGTCC-3′ and 5′-GGCCCCATTTTGCCATTTTTATTTAG-3′
Atg8a (CG32672):
5′-TCGCAAATATCCAGACCGTGTGCCCGTC-3′ and 5′-GCCGATGTTGGTGGAATGACGTTGTTCAC-3′

Image Analysis

For image analysis, single-channel confocal images were converted into grayscale and the number and area of protein aggregates was measured in an automated way with the "Analyze Particle" function of ImageJ on the basis of polyubiquitin immunoreactivity. A cut-off of 10 pixels was applied to exclude background staining from the analysis. A similar approach was used to count vesicles.

In immunoelectron microscopy images, the total number of gold particles was counted to estimate the presence of protein aggregates.

Quantification of the intensity of antibody staining was done by measuring the mean fluorescence intensity with the Histogram function of Photoshop (Adobe) in single confocal images taken with the same settings.

Transmission and Immunogold-Electron Microscopy

For transmission electron microscopy (TEM), thoraces were dissected and incubated in fixative (2% formaldehyde, 2.5% glutaraldehyde and 0.06% picric acid in 100 mM cacodylate buffer, pH 7.2) and processed as previously described (Bai et al., 2007).

For immunogold-electron microscopy, thoraces were fixed for 40 min in 0.1% Triton X-100 and 4% paraformaldehyde in 0.1M Sodium Phosphate buffer pH 7.4 and embedded in LR White resin (Electron Microscopy Sciences). ~80 nm thick LR White sections were picked up on formvar/carbon coated copper grids for immunolabeling.

The gold-labeling was carried out at room temperature on a piece of parafilm. Anti-ubiquitin (1:50 P4D1, Cell Signaling) antibodies and protein A gold were diluted in PBS with 0.1% Triton X-100 and 1% BSA. The diluted antibody solution was centrifuged 1 min at 14000 rpm prior to labeling to avoid possible aggregates. Grids were floated on drops of PBS with 0.1% Triton X-100 and 1% BSA for 10 min to block for unspecific labeling, transferred to 5µl drops of primary antibody and incubated for 30 min. The grids were then washed in 4 drops of PBS for a total of 15 min, transferred to 5µl drops of Protein-A gold for 20 min, washed in 4 drops of PBS for 15 min and 6 drops of double distilled water. Grids were picked up with metal loops and the excess liquid was removed by streaking on a filter paper. Post-staining of the LR White sections was done with 0.3% lead citrate. The grids were examined in a TecnaiG^2 Spirit BioTWIN mission electron microscope and images were recorded with an AMT 2k CCD camera (courtesy of Maria Ericsson, Harvard Medical School EM Facility).

Western Blot and Biochemical Analysis of Detergent-Insoluble Fractions

Biochemical Analysis of detergent-insoluble fractions was done as previously (Cumming et al., 2008; Nezis et al., 2008; Tofaris et al., 2003). In brief, either fly heads and abdomens, or thoraces were dissected from at least 15 male flies and homogenized in ice-cold PBS with 1% Triton X-100 containing protease and phosphatase inhibitors. Homogenates were centrifuged at 14000 rpm at 4°C and supernatant collected (Triton X-100 soluble fraction). The remaining pellet was washed in ice-cold PBS with 1% Triton X-100. The pellet was then resuspended in RIPA buffer containing 8M urea and 5% SDS, centrifuged at 14000 rpm at 4°C, and collected supernatants (Triton X-100 insoluble fraction) were analyzed on 4%–20% SDS-PAGE. Western blots were probed with anti-ubiquitin antibodies (P4D1, Cell Signaling; 1:1000) and either anti-α-Tubulin or anti-Histone H3 antibodies (Cell Signaling, 1:1000) as loading controls.

For densitometry of western blots, band intensity was quantified with the Histogram function of Photoshop.

SUPPLEMENTAL REFERENCES

Bai, J., Hartwig, J. H., and Perrimon, N. (2007). SALS, a WH2-domain-containing protein, promotes sarcomeric actin filament elongation from pointed ends during Drosophila muscle growth. Dev. Cell *13*, 828-842.

Clyne, P. J., Brotman, J. S., Sweeney, S. T., and Davis, G. (2003). Green fluorescent protein tagging Drosophila proteins at their native genomic loci with small P elements. Genetics *165*, 1433-1441.

Cumming, R. C., Simonsen, A., and Finley, K. D. (2008). Quantitative analysis of autophagic activity in Drosophila neural tissues by measuring the turnover rates of pathway substrates. Methods Enzymol. *451*, 639-651.

Curran, S. P., Wu, X., Riedel, C. G., and Ruvkun, G. (2009). A soma-to-germline transformation in long-lived *Caenorhabditis elegans* mutants. Nature *459*, 1079-1084.

Hess, N. K., Singer, P. A., Trinh, K., Nikkhoy, M., and Bernstein, S. I. (2007). Transcriptional regulation of the *Drosophila melanogaster* muscle myosin heavy-chain gene. Gene Expr. Patterns *7*, 413-422.

Huang, H., Potter, C. J., Tao, W., Li, D. M., Brogiolo, W., Hafen, E., Sun, H., and Xu, T. (1999). PTEN affects cell size, cell proliferation and apoptosis during Drosophila eye development. Development *126*, 5365-5372.

Miron, M., Verdu, J., Lachance, P. E., Birnbaum, M. J., Lasko, P. F., and Sonenberg, N. (2001). The translational inhibitor 4E-BP is an effector of PI(3)K/Akt signaling and cell growth in Drosophila. Nat. Cell Biol. *3*, 596-601.

Puig, O., Marr, M. T., Ruhf, M. L., and Tjian, R. (2003). Control of cell number by Drosophila FOXO: downstream and feedback regulation of the insulin receptor pathway. Genes Dev. *17*, 2006-2020.

Pulipparacharuvil, S., Akbar, M. A., Ray, S., Sevrioukov, E. A., Haberman, A. S., Rohrer, J., and Kramer, H. (2005). Drosophila Vps16A is required for trafficking to lysosomes and biogenesis of pigment granules. J. Cell Sci. *118*, 3663-3673.

Ranganayakulu, G., Schulz, R. A., and Olson, E. N. (1996). Wingless signaling induces nautilus expression in the ventral mesoderm of the Drosophila embryo. Dev. Biol. *176*, 143-148.

Schuster, C. M., Davis, G. W., Fetter, R. D., and Goodman, C. S. (1996). Genetic dissection of structural and functional components of synaptic plasticity. I. Fasciclin II controls synaptic stabilization and growth. Neuron *17*, 641-654.

Teleman, A.A., Hietakangas, V., Sayadian, A. C., and Cohen, S. M. (2008). Nutritional control of protein biosynthetic capacity by insulin via Myc in Drosophila. Cell Metab. *7*, 21-32.

Tofaris, G. K., Razzaq, A., Ghetti, B., Lilley, K. S., and Spillantini, M. G. (2003). Ubiquitination of alpha-synuclein in Lewy bodies is a pathological event not associated with impairment of proteasome function. J. Biol. Chem. *278*, 44405-44411.

Zheng, X., Yang, Z., Yue, Z., Alvarez, J. D., and Sehgal, A. (2007). FOXO and insulin signaling regulate sensitivity of the circadian clock to oxidative stress. Proc. Natl. Acad. Sci. USA *104*, 15899-15904.
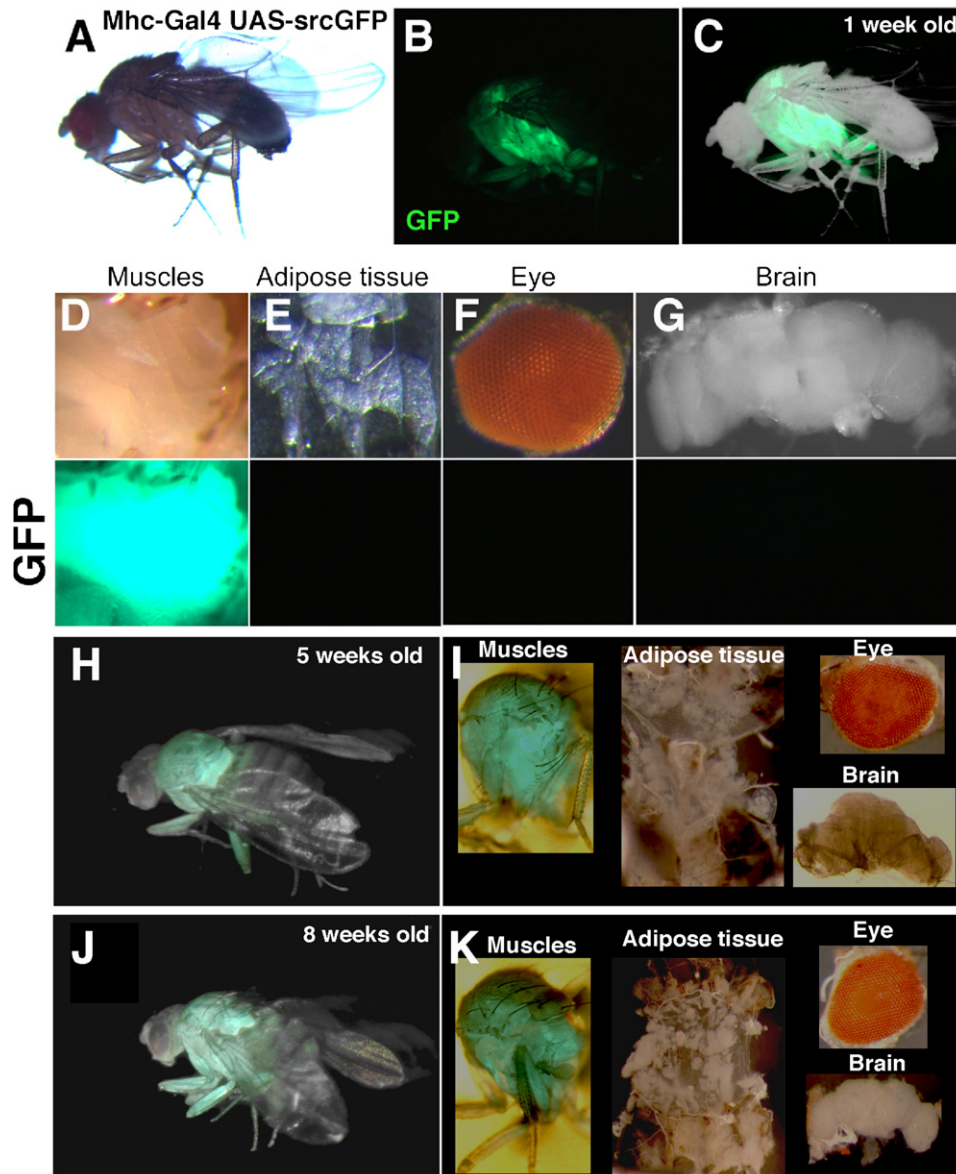
Figure S1. Mhc-Gal4 Drives Transgene Expression Specifically in Muscles, Related to Figure 1 and Figure 6

(A–D) Overview of flies overexpressing *EGFP* with the Mhc-Gal4 driver (*UAS-srcEGFP*/+ *Mhc-Gal4*/+; magnification is 10x). GFP fluorescence (green) is detected to identify the tissues where Mhc-Gal4 can drive transgene expression. (A and D) Strong GFP fluorescence is detected in muscles of the thorax (direct and indirect flight muscles) and in leg muscles. Weaker GFP fluorescence is detected in head and abdominal muscles (not shown).

(E–G) In *UAS-srcEGFP*/+ *Mhc-Gal4*/+ flies, no EGFP fluorescence is detected in the adipose tissue (E, peripheral fat body of the abdomen), the eye (F), and the brain (G). Similar results were obtained by driving the expression of other transgenes encoding GFP-tagged proteins (not shown).

(H–K) Transgene expression is maintained with age specifically in muscles, as assessed by monitoring GFP expression at 5 (H–I) and 8 weeks (J–K) of age. No GFP expression was detected in nonmuscle tissues (H–K).

Altogether, these observations indicate that Mhc-Gal4 drives transgene expression specifically in skeletal muscles but not in other tissues, including the adipose tissue, retina, and brain. This observation is consistent with previous studies reporting that *Mhc* is specifically expressed in muscles and that Mhc-Gal4 is a muscle specific Gal4 driver (Demontis and Perrimon, 2009; Hess et al., 2007; Schuster et al., 1996).
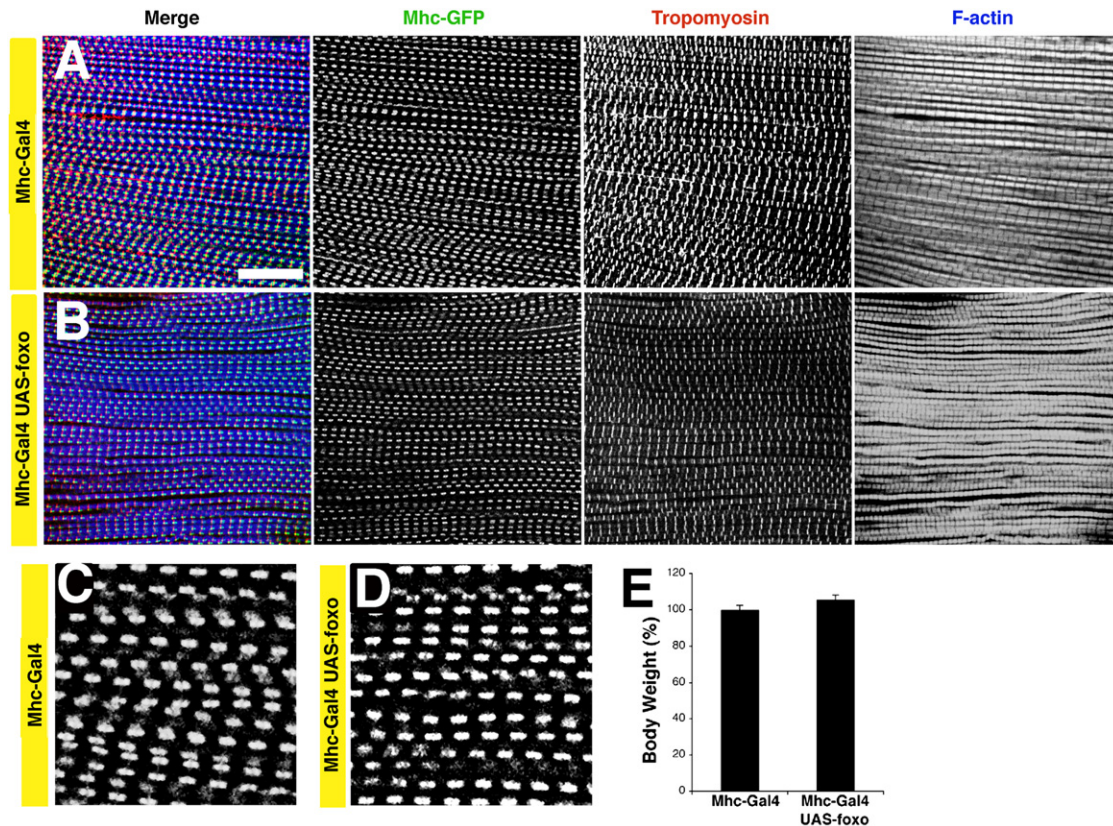
Figure S2. Mhc-Gal4 Drives *foxo* Overexpression in Muscles without Affecting Developmental Growth and Differentiation, Related to Figure 1

(A–D) Staining of indirect flight muscles with phalloidin (F-actin) and anti-Tropomyosin antibodies, and Mhc-GFP (WeeP26) fluorescence. The distribution of the sarcomeric components F-actin, Tropomyosin, and Mhc is similar in *Mhc-Gal4/Mhc-GFP* and *UAS-foxo/+ Mhc-Gal4/Mhc-GFP* flies, indicating that muscle differentiation and sarcomere assembly are unaltered. Scare bar, 20 μm. (C–D) Higher magnification panels display Mhc-GFP fluorescence of *Mhc-Gal4/Mhc-GFP* and *UAS-foxo/+ Mhc-Gal4/Mhc-GFP* flies.

(E) *foxo* overexpression does not substantially affect developmental growth, as estimated by measuring the variation (%) in average body weight of 1-week-old flies (n[flies per batch] = 25, n[batch] = 2; standard deviation is indicated).
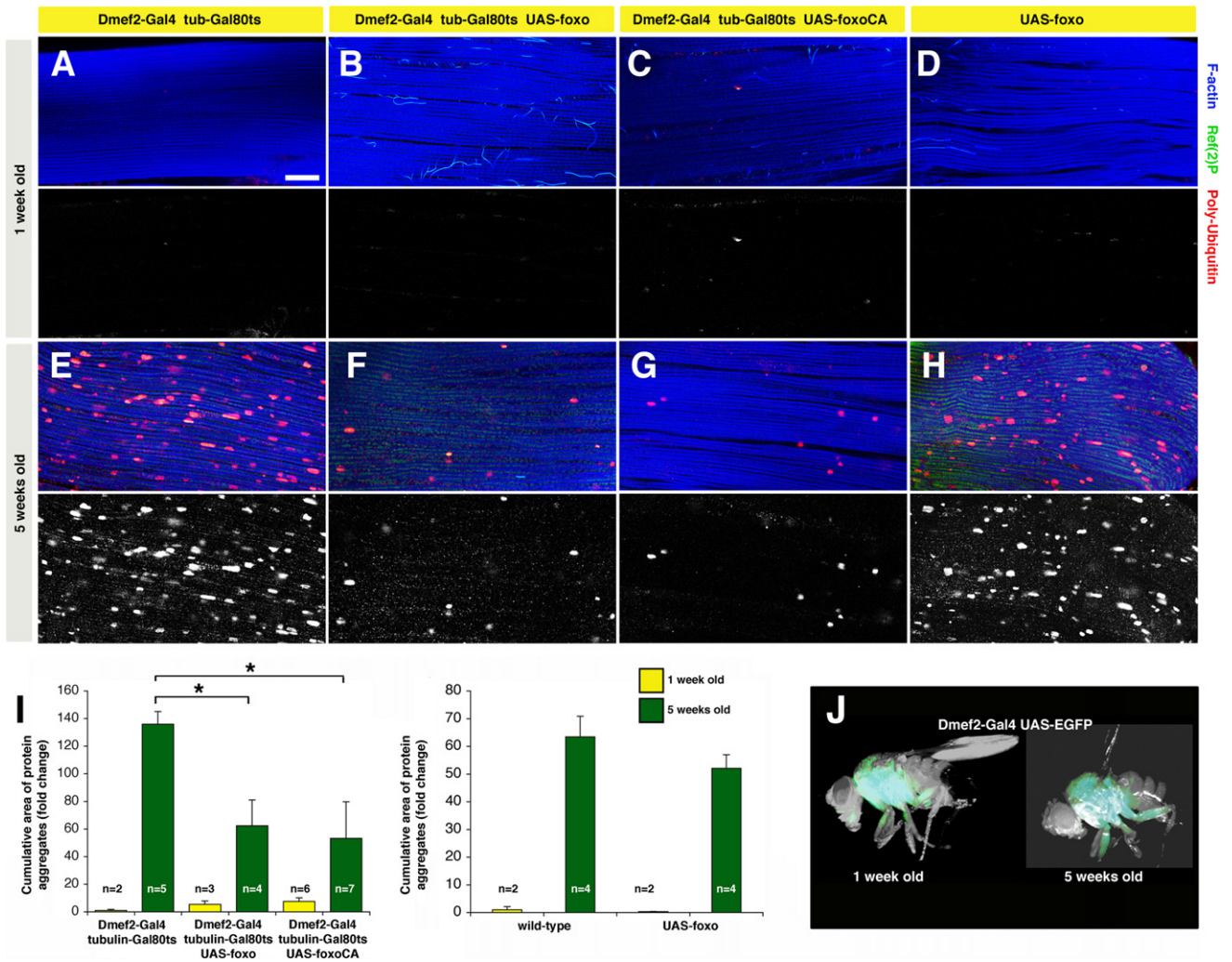
Figure S3. Overexpression in Adulthood of Wild-Type and Constitutive Active *foxo* Preserves Muscle Proteostasis, Related to Figure 1 and Figure 2

(A–H) Staining of indirect flight muscles with overexpression of either wild-type or constitutive active (ca) *foxo*. Transgene expression is temporally controlled with the temperature sensitive tubulin-Gal80^{ts} to achieve adult onset transgene expression with the muscle Dmef2-Gal4 driver at 29°C. Overexpression of both wild-type (B and F) and constitutive active *foxo* (C and G) results in preservation of proteostasis, as exemplified by decreased deposition of protein aggregates (Poly-ubiquitin and Ref(2)P immunoreactivities) at 5 weeks of age, in comparison with controls (the Dmef2-Gal4 driver [A and E], and the UAS-foxo transgene alone)D and H]). Scale bar is 20 μm.

(I) Fold change in the cumulative area of protein aggregates at 1 (yellow) and 5 (green) weeks of age from muscles of different animals indicates significant preservation of proteostasis in response to overexpression of wild-type or constitutive active *foxo* (*p < 0.05; SEM is indicated with n).

(J) Dmef2-Gal4 drives transgene expression specifically in all muscles (including thoracic and abdominal muscles) at both 1 and 5 weeks of age.

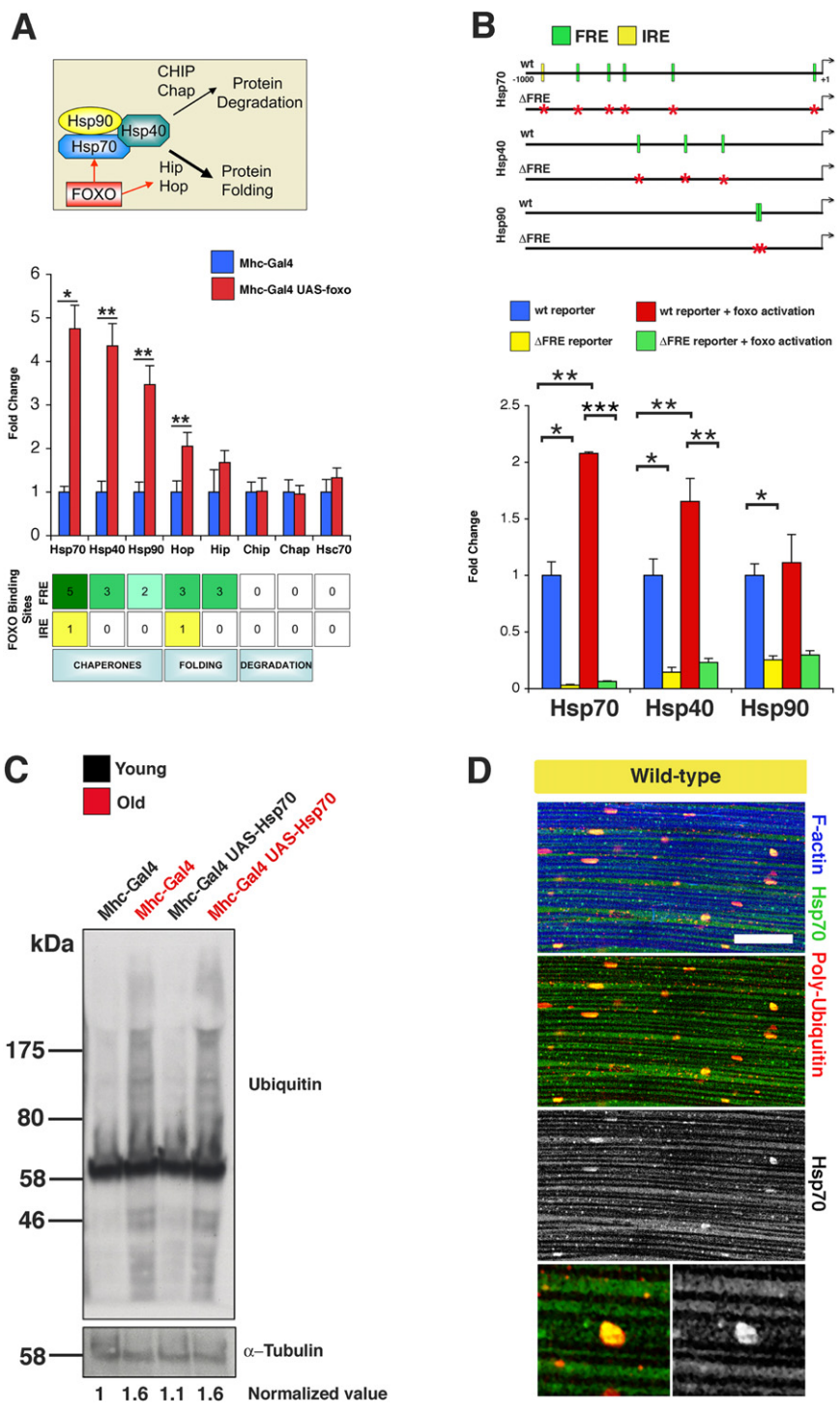**Figure S4. FOXO Induces the Expression of *Hsp70* and Associated Folding Cochaperones, Related to Figure 2**

(A) Hsp70 is a key player in proteostasis via its association with co-chaperones (Hsp40 and Hsp90) and co-factors involved in protein folding (Hip and Hop) and degradation (CHIP and Chap). The mRNA levels of *Hsp70* increase in thoracic muscles at 1 week of age in response to *foxo* overexpression (red; *UAS-foxo*/+; *Mhc-Gal4*/+) in comparison with controls (blue; *Mhc-Gal4*/+). A significant increase is also detected in the mRNA levels of the co-chaperones *Hsp40* and *Hsp90* and co-factors involved in protein folding (*Hop*) but not in protein degradation (*Chip*, *Chap*) and *Hsc70*. Error bars represent SEM with n = 4 and *p < 0.05; **p < 0.01. Regulated genes have several putative FOXO binding sites (numbers in box) in their proximal (1 kb) promoter region (green: Fork-head Responsive Element (FRE); yellow: Insulin Responsive Element [IRE]).

(B) Luciferase assays in cell culture using wild-type (wt) and mutant versions (ΔFRE) of the promoter regions of FOXO-regulated chaperones. Green and yellow

boxes indicate FREs and IREs in wild-type (wt) reporters, respectively, while a red star denotes mutation of a FOXO binding site in the mutant version of the promoter (arrow denotes ATG). (B) Relative Luciferase activity of wt and ΔFRE mutant reporters, normalized to an *actin5c* promoter-based Luciferase reporter. *Foxo* overexpression increases the transcriptional activity of the wt Luciferase reporters, which is suppressed by the removal of FOXO binding sites (ΔFRE mutant reporters). Error bars represent sem with n = 4 and *p < 0.05; **p < 0.01; ***p < 0.001. Table S2 provides information on the promoter regions used for the construction of Luciferase reporters.

(C) Western blot analysis of Triton X-100 insoluble fractions from thoraces of syngenic flies with or without *Hsp70* overexpression in muscles. Thoraces from young flies (1 week old, black) are compared with thoraces from old flies (6 weeks old, red). Note a similar deposition of Ubiquitin-conjugated proteins in old flies independent of *Hsp70* overexpression. Quantification of ubiquitin-conjugated proteins levels normalized to Tubulin levels is indicated (normalized value).

(D) Immunostaining of indirect flight muscles from wild-type old flies (5 weeks of age) with an anti-Hsp70 antibody. Hsp70 immunoreactivity (green) is detected in the cytoplasm of young flies (not shown) and old flies, where it is additionally detected in polyubiquitin protein aggregates (red). Association of Hsp70 with protein aggregates may possibly decrease their toxicity (proteotoxicity). F-actin (blue, phalloidin staining) identifies myofibrils. Scale bar is 20 μm.
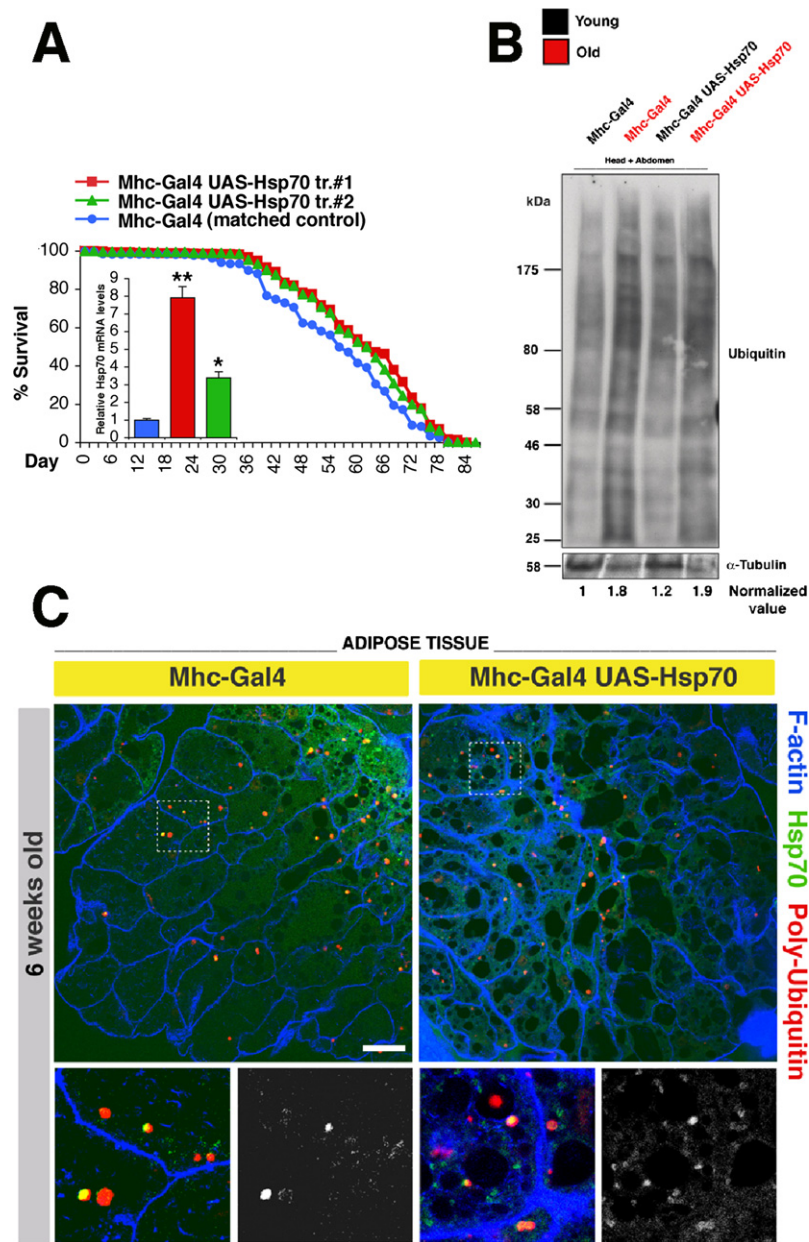
Figure S5. Minor Contribution of *Hsp70* Overexpression in Muscles to the Systemic Regulation of Aging, Related to Figure 4 and Figure 6

(A) *Hsp70* overexpression has a partial effect on muscle function (not shown) and life span in comparison with syngenic control flies. Median and maximum life span: *Mhc-Gal4/+* = 56 and 80 days (n = 774); *Mhc-Gal4/UAS-Hsp70* = 62 and 84 days (n = 626); p < 0.01). Relative *Hsp70* mRNA levels are detected in thoraces from control (blue) and *Hsp70* overexpressing (red and green) flies by qPCR (sem is indicated with n = 4; *p < 0.05 and **p < 0.01).

(B and C) Accumulation of polyubiquitinated proteins in nonmuscle tissues of flies overexpressing *Hsp70* in Muscles. (B) Western blot of Triton X-100 insoluble fractions from abdominal and head tissues of syngenic flies with or without *Hsp70* overexpression in muscles (*Mhc-Gal4/+*; and *Mhc-Gal4/UAS-Hsp70*) at 1 (young) and 6 weeks (old) of age. Note a similar accumulation of Ubiquitin-conjugated proteins with age, indicating that *Hsp70* overexpression in muscles is not sufficient per se to mitigate the loss of proteostasis in non-muscle tissues. Normalized values (based on α-Tubulin levels) are shown.

(C) Immunostaining of adipose tissue (peripheral fat body of the abdomen) from flies with or without *Hsp70* overexpression in muscles at 6 weeks of age. Hsp70 immunoreactivity (green) is detected in the cytoplasm and associated with some polyubiquitin protein aggregates (red) that accumulate in both conditions. F-actin staining is shown in blue. Scale bar, 20 μm.
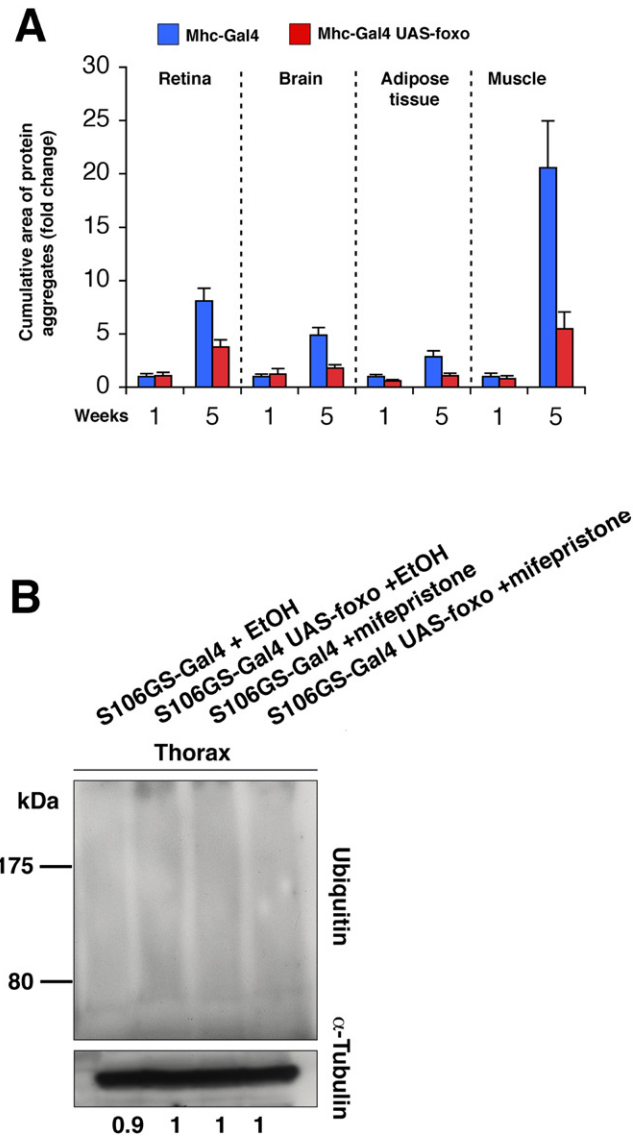
Figure S6. Prominence of Muscle Aging Is Seemingly Not Affected by *foxo* Overexpression in the Abdominal Fat Body, Related to Figure 6

(A) Age-related changes in the cumulative area of protein aggregates are more prominent in muscles in comparison with other tissues (data displayed are from Figure 1 and Figure 6).

(B) Western blot analysis of Triton X-100 insoluble fractions from 5 weeks old S106GS-Gal4 flies at 29°C, with or without the UAS-foxo transgene, and either ethanol (EtOH, mock) or the inducer of expression mifepristone (S106GS-Gal4 is dependent on this progesterone analog to drive UAS-construct expression in the fat body (Giannakou et al., 2004; Hwangbo et al., 2004)). FOXO activation in the fat body may regulate systemic proteostasis, although no substantial difference in the deposition of protein aggregates in muscles (thoraces) is observed in the various conditions tested.
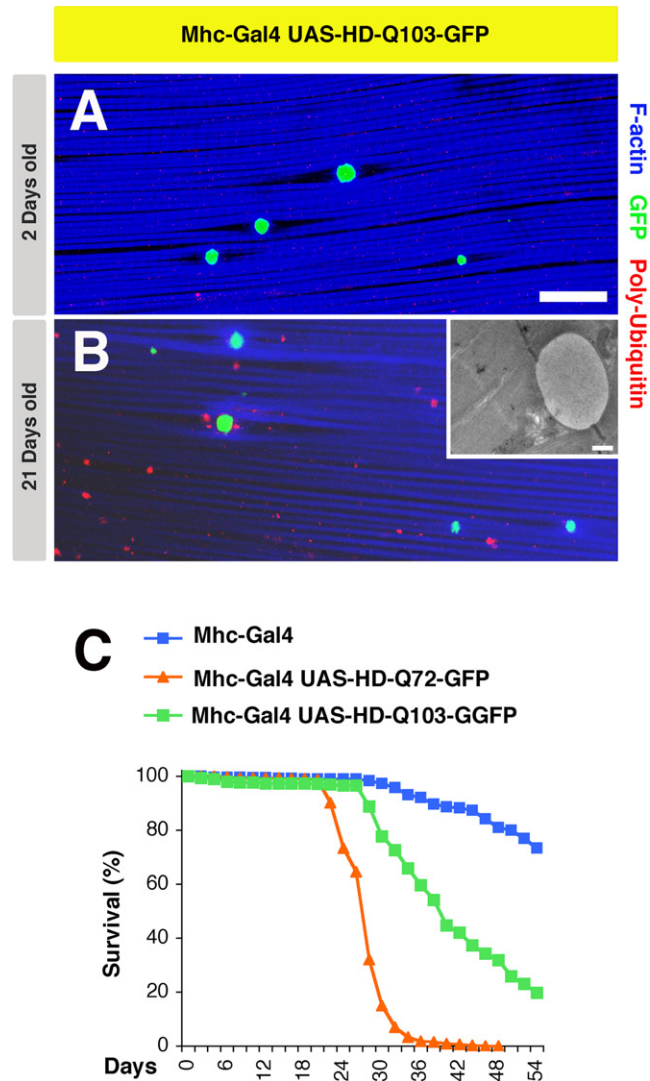
Figure S7. Expression of Mutant Human Huntington's Disease Proteins in Muscles Is Sufficient to Decrease Life Span, Related to Figure 4 and Figure 7

(A and B) GFP-positive protein aggregates are detected in muscles from both young (2 days old) and older flies (21 days old) upon overexpression in muscles of GFP-tagged, aggregation-prone human Huntington's disease proteins. Note that Huntington's disease protein aggregates are distinct from aggregates of endogenous damaged proteins (identified via polyubiquitin immunoreactivity, red) in both confocal and transmission electron microscopy (inset in B). Scale bars, 20 μm (A, confocal microscopy) and 500 nm (inbox in B, electron microscopy).

(C) Overexpression of Huntington's disease proteins in muscles is sufficient to decrease life span, indicating that muscle proteostasis is limiting for life expectancy (p < 0.001, with n[*Mhc-Gal4*/+] = 1264, n[*UAS-HD-Q72-GFP*/+; +/+; *Mhc-Gal4*/+] = 372, and [*UAS-HD-Q103-GFP*/+; +/+; *Mhc-Gal4*/+] = 490).